이학박사 학위논문

The role of haptoglobin in osteoclastogenesis

파골세포 분화에 대한 합토글로빈의 역할

2017년 2월

서울대학교 대학원
치의과학과 세포 및 발생생물학 전공
진 원 종

파골세포 분화에 대한 합토글로빈의 역할

지도교수 이 장 희

이 논문을 이학박사학위논문으로 제출함

2016 년 10월

서울대학교 대학원

치의과학과 세포및발생생물학 전공

진 원 종

진원종의 박사학위논문을 인준함

2016 년 12 월

위 원 장 성노현 (인)

부 위 원 장 이장희 (인)

위 원 김홍희 (인)

위 원 이승복 (인)

위 원 김대원 (인)

The role of haptoglobin in Osteoclastogenesis

by

Won Jong Jin

Advisor:

Prof. Zang Hee Lee, D.D.S., Ph.D

A thesis Submitted in Partial Fulfillment of the
Requirements for the Degree of Doctor of Philosophy

December, 2016

Doctoral Committee:

Professor _____,Chairman

Professor _____,Vice chairman

Professor _____

Professor _____

Professor _____

Abstract

The role of haptoglobin in osteoclastogenesis

Won Jong Jin

Department of Cell and Developmental Biology

The Graduate School

Seoul National University

(Directed by Prof. Zang Hee Lee, D.D.S., Ph.D)

Haptoglobin (Hp), a member of the acute phase proteins, is known to be a major hemoglobin (Hb)-binding protein that plays a protective role against Hb-induced cytotoxicity in various organs. Hp is primarily expressed in hepatocytes, and recent studies have shown its expression in other cells, such as keratinocytes, leucocytes, fibrocytes and adipocytes. However, the involvement of Hp in bone-related cells has not been fully understood. In this study, I

investigated the effects of Hp in osteoclastogenesis and skeletal health. Inflammatory cytokines, interleukin-1α (IL-1α), tumor necrosis factor α (TNF-α) and lipopolysaccharide (LPS) induced Hp secretion in the bone-forming cells, osteoblasts. Histo-morphometric analyses indicated that the deletion of Hp gene showed significant bone loss with increasing osteoclast formation. Administration of Hp in Hp knockout ($Hp^{-/-}$) mice stimulated a higher bone volume increment than that in PBS-injected mice. Consistent with the *in vivo* results, IL-1α-induced osteoclast formation by co-culture of Hp null calvarial osteoblast and wild-type (WT) bone marrow-derived macrophages (BMMs) showed increase higher osteoclastogenesis than that observed in WT osteoblast *in vitro*. Stimulation of Hp inhibited osteoclastogenesis by suppression of major transcription factors such as c-Fos and NFATc1 expression. Overexpression of c-Fos in osteoclast precursor cells rescued Hp-mediated suppression of osteoclastogenesis with promotion of its down-stream master transcription factor, NFATc1. I found that Hp-induced suppression of c-Fos expression was mediated by an increase in interferon beta (IFNβ) levels, a well-known c-Fos inhibitor. Hp-induced inhibition of osteoclastogenesis substantially recovered following treatment with IFNβ-specific neutralizing antibody and IFN-type I receptor knockout cells. In addition, I determined that Hp-induced IFNβ expression was activated via toll-like receptor 4 (TLR4). Flow cytometer

analysis showed that stimulation of Hp or the well-known TLR4 ligand, LPS induced TLR4 internalization. Furthermore, a binding assay for TLR4 showed direct interaction of Hp to TLR4 when I compared to that of bovine serum albumin (BSA) interaction. Taken together, these results demonstrate that inflammation-induced secreted-Hp from osteoblast plays a protective role against excessive osteoclastogenesis via the TLR4-IFNβ signaling pathway.

Key words : Hp, osteoblast, osteoclast, c-Fos, TLR4, IFNβ

Student number : 2009-21937

CONTENTS

LIST OF FIGURES

LIST OF TABLES

ABBREVIATIONS

M-CSF	Macrophage-colony stimulating factor
RANKL	Receptor activator of nuclear factor κB (NF-κB) ligand
OPG	Osteoprotegrin
BMMs	Bone marrow-derived macrophages
Hp	Haptoglobin
Hb	Hemoglobin
IL-1	Interleukin-1
IFNβ	Interferon beta
TNFα	Tumor necrosis factor alpha
NFATc1	Nuclear factor of activated T cell c1
TRAP	Tartrate-resistant acid phosphatase
MAPK	Mitogen-activated protein kinase
TLRs	Toll-like receptors
LPS	Lipopolysaccharide

I. Introduction

I.1. Bone remodeling and diseases

Bone is a metabolically active organ that continuously undergoes resorption and renewal during lifetime. The bone homeostasis is mainly regulated by a delicate balance of bone cells—osteoblasts and osteoclasts (Fig. 1). This process, termed "remodeling" is mainly achieved by coupling of osteoblasts and osteoclasts which facilitates various functions, including mechanical support, protection for tissues, calcium release, and hematopoiesis (Rodan, 1998). Several factors such as ephrin B2/EphB4, Semaphorin 4D/PlexinB1, and Ephhrin A2/EphA2 interaction have been proposed as osteoblast and osteoclast coupling factors (Irie et al., 2009; Negishi-Koga et al., 2011; Zhao et al., 2006). Disparity in processing between osteoblasts and osteoclasts results in pathological bone diseases such as osteoporosis, Paget's disease, and rheumatoid arthritis (Manolagas and Jilka, 1995). These osteoporotic diseases are well characterized by excessive osteoclast activation over osteoblast-mediated bone formation, which has been shown to result in loss of bone quantity and quality. Thus, understanding of this coupling mechanism is required to take measures to ensure appropriate bone mass maintenance and limit its pathophysiological role in bone-related disorders. According to the

report of Korean Society for Bone and Mineral Research (KSBMR), 50% of patients with osteoporosis and femur shaft fractures are unable to recover to original mobility. The patient mortality has reached an intra-annual rate of 20% (KSBMR, 2015). Therefore, the molecular basis of osteoclast activation needs to be investigated in order to prevent bone fragility and increase the quality of life.

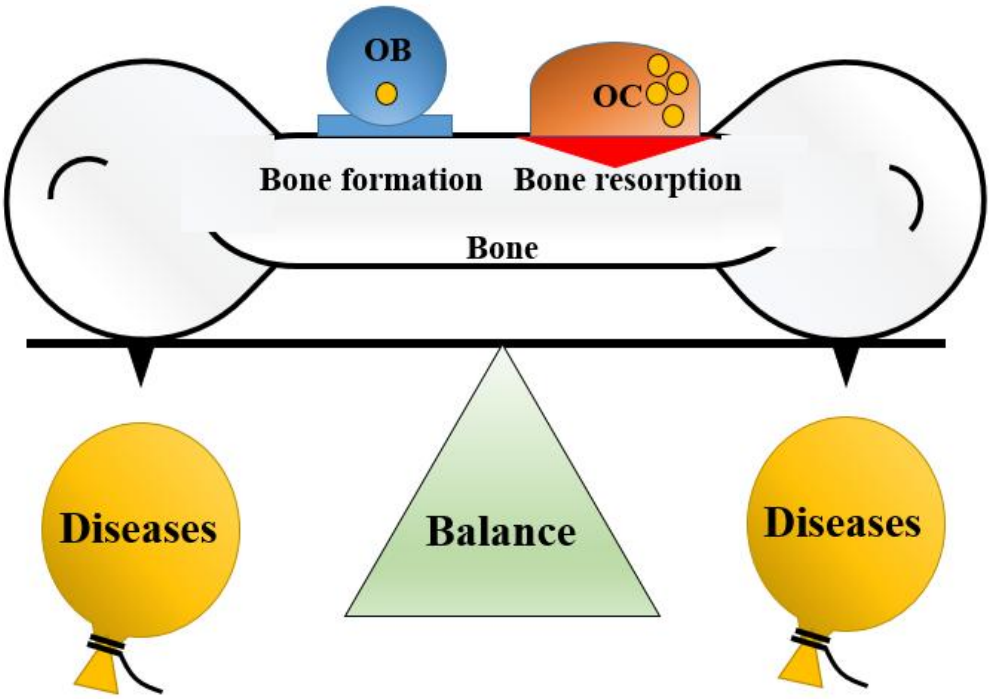

Figure 1. Bone resorption by osteoclast and bone formation by osteoblast maintained a balance to prevent pathological bone diseases. Bone is continuously remodeled, with a balance maintained between osteoclasts and osteoblasts. Disruption of this balance provokes pathological bone diseases and osteopetrotic or osteoporotic disorders.

I.2. Osteoclastogenesis and RANKL-signaling

Osteoclasts—the multinucleated bone resorptive cells—originated from monocyte/macrophage lineage cells in which osteoclast differentiation is mainly induced by cytokines, macrophage colony stimulating factor (M-CSF), and receptor activator of NF-κB ligand (RANKL) (Kodama et al., 1991; Lacey et al., 1998). Indeed, the interaction between RANKL and it receptor RANK plays a key role in osteoclast differentiation through sequential steps of polarization-fusion-maturation, while M-CSF is considered as an essential factor for the survival and induction of RANK expression on osteoclast precursor cells (Arai et al., 1999). RANKL is a member of the tumor necrosis factor (TNF) receptor family that is expressed on bone marrow stromal cells and osteoblasts resulting from stimulation by several inflammatory cytokines, such as IL-1, IL-6, TNFα and lipopolysaccharide (LPS) (Collin-Osdoby et al., 2001). Thereby, inflammatory factors contribute to osteoclastogenesis from its precursor cells through induction of RANKL on osteoblasts.

Signal transduction by RANKL/RANK-binding induced recruitment of TNF receptor-associated factor 6 (TRAF6), consistently activates various downstream signaling pathways, including nuclear factor-kappa B (NF-κB), mitogen-activated protein kinases (MAPKs), and calcium signaling pathway. Under RANKL stimulation, TRAF6 activates a complex consisting of IκB

kinase (IKK) to induce the phosphorylation and degradation of Inhibitor of kappa B (IκB), which releases P65/P50 heterodimers for translocation into the nucleus. Therefore, the activation of the canonical NF-κB signaling pathway results in the expression of c-Fos, an early stage transcription factor, and its downstream target, nuclear factor of activated T-cell, cytoplasmic 1 (NFATc1), both of which are important transcription factors for osteoclastogenesis (Boyce et al., 2015). The RANK-TRAF6 binding induces the activation of phospholipase C gamma (PLCγ)-calcium signaling for Ca^{2+}-dependent NFATc1 regulation. Signaling via MAPKs-JNK, ERK and P38-is also involved in the activation of c-Fos and NFATc1 in osteoclastogenesis (Soysa et al., 2012) (Fig. 2). Indeed, it has been reported that forced expression of NFATc1 promotes osteoclastogenesis without RANKL stimulation in precursor cells (Takayanagi et al., 2002a). Therefore, RANKL-induced NFATc1 is considered as the master transcription factor for osteoclastogenesis from bone marrow-derived macrophages (BMMs), the precursor cells. Consequently, the transcription factor NFATc1 regulates not only osteoclast-specific genes including tartrate-resistant acid phosphatase (TRAP), cathepsin K, and osteoclast-associated receptor (OSCAR), but also matrix metalloproteinases (MMPs). Thus, the expression of NFATc1 target genes confers bone resorptive functions to osteoclasts (Nakashima and Takayanagi, 2011).

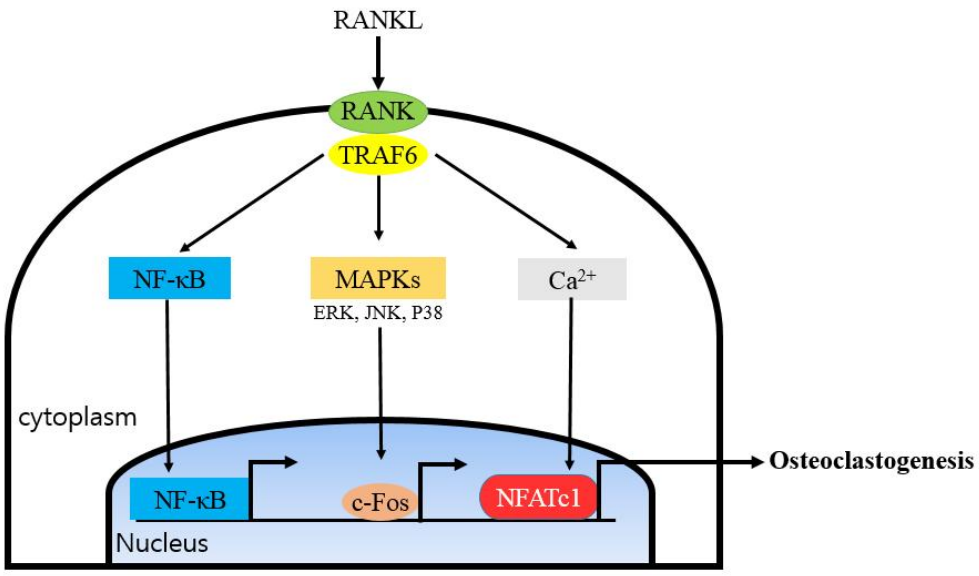

Figure 2. RANKL-induced intracellular signaling network of osteoclast differentiation. The binding of RANKL to its receptor RANK induces the recruitment of TRAF6, an adaptor molecule, in the cytoplasm. This interaction leads to the activation of various intracellular signaling cascades, such as the NF-κB, MAPKs, and calcium signaling cascades. RANKL-induced dissociation of IκB from NF-κB results in nuclear translocation of NF-κB to regulate c-Fos and NFATc1. RANKL-induced activation of MAPKs, such as ERK, JNK, and P38, activates the transcription factor c-Fos. The key transcription factor NFATc1, localized to the nucleus by Ca^{2+} signaling, is also activated by NF-κB and MAPKs signaling activation. These signaling complexes affect autoamplification of NFATc1, leading to the transcription of osteoclast-specific

genes.

I.3. Haptoglobin

Haptoglobin (Hp) is an abundant plasma glycoprotein identified by Plononovski and Jayle (1938) (Raynes et al., 1991). Hp is mainly synthesized by hepatocytes in liver and is released into the blood. At sites of injury, IL-6 is released by leukocyte and delivered to liver via the blood stream to stimulate expression of Hp in hepatocytes (Heinrich et al., 1990). The fundamental role of Hp is to bind to hemoglobin (Hb) released as a result of erythrocyte hemolysis and thereby to protect toxic Hb-induced oxidative stress and inflammation (Tseng et al., 2004). Erythrocytes can rupture during several pathological conditions, such as autoimmune disorders, malaria, hemoglobinopathies, and infections (Rother et al., 2005). Therefore, extracellular Hb, originating from hemolysis of RBCs, continuously undergoes autoxidation, which produces superoxide that then dismutates into hydrogen peroxide (H_2O_2) (Rifkind et al., 2014). The resulting superoxide, H_2O_2, and the reactive oxygen species (ROS) subsequently induce oxidative stress in cells. These oxidative reactions contribute to pathological conditions, including sickle cell disease, kidney dysfunction, atherosclerosis, and hemolytic anemia (Rifkind et al., 2014). Therefore, Hb-Hp binding has been shown to play a protective role against Hb-induced tissue damage. It is well known that the Hb-Hp complex binds to the

CD163 scavenger receptor on the surfaces of macrophages and monocytes (Kristiansen et al., 2001). Hb-Hp-induced CD163 internalization leads to the enzymatic activation of heme oxygenase (HO), which degrades the hemoglobin subunit, heme into biliverdin, which is converted to carbon monoxide, bilirubin, and free iron; this restores cellular homeostasis. Hp has also been reported to be associated with high glucose tolerance, glucose-stimulated insulin secretion, and adiponectin expression (Lisi et al., 2011). This group showed that insulin-induced phosphorylation of the AKT S473 was higher in the liver, skeletal muscle, and white adipose tissue of Hp-deficiency mice than in the same tissues in wild type mice. Bertaggia et al showed downregulation of antioxidants expression in the tibialis anterior muscle of Hp-deficient mice and that the absence of Hp affects muscle force generation and resistance to fatigue (Bertaggia et al., 2014). In addition, they also showed impaired antioxidant response and exacerbated oxidative stress in Hp-deficient mice. Collectively, these data indicate that Hp plays a pivotal role in various tissue metabolic activities and functions (Fig. 3). However, the precise molecular mechanisms of Hp-induced cellular signaling remains poorly understood.

In addition to liver, several recent studies demonstrated that Hp is expressed in other tissues, such as lung, skin, and kidney (D'Armiento et al., 1997). Furthermore, Hp participates in adiposity, new vessels formation, fibroblast

migration, and graft rejection (Cid et al., 1993; de Kleijn et al., 2002; Maffei et al., 2016; Shen et al., 2015). Importantly, El-Ghmati et al showed that Hp binds to a various immune cells, including monocytes, granulocytes, and natural killer cells via CD11b/CD18 receptor (El Ghmati et al., 1996). Another group revealed that Hp binds to B lymphocytes through CD22 (Hanasaki et al., 1995). The binding of Hp to CD22, inhibited signaling induced by other ligands and consequently negatively regulated the B lymphocyte function. More interestingly, a recent study showed that Hp can bind to chemokine (C-C motif) receptor 2 (CCR2) (Maffei et al., 2009). The authors of this study observed that Hp stimulation (treatment at 50 or 100 μg/ml) induced monocyte migration through binding with CCR2 and internalized CCR2-mediated activation of its downstream signal transducer ERK phosphorylation. Collectively, these previous reports suggest that Hp has the potential to bind with several receptors apart from Hb, thereby carrying out numerous biological functions.

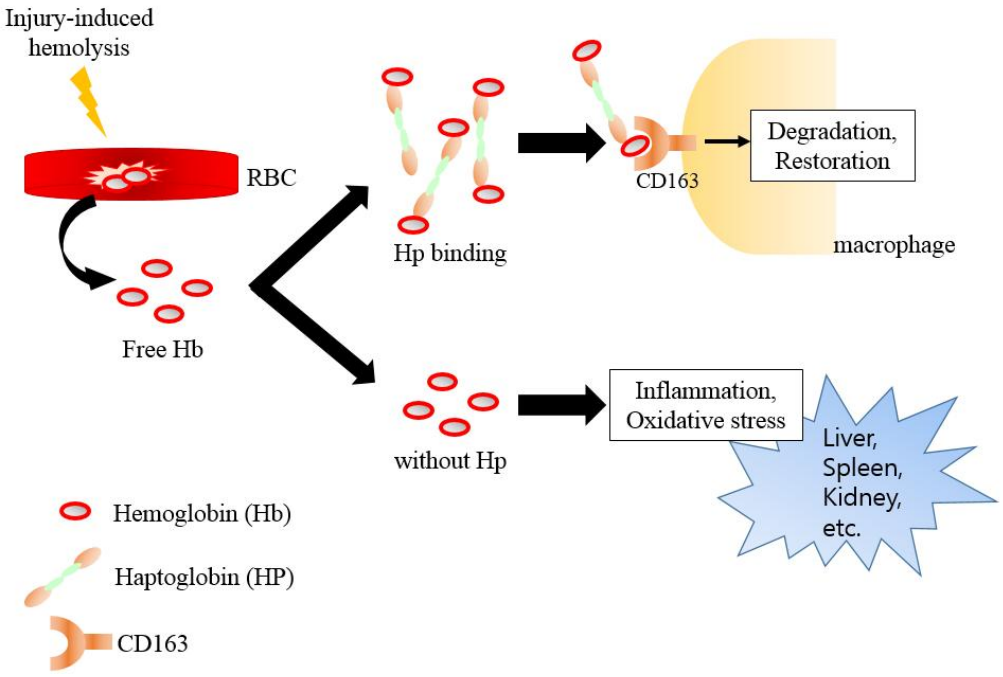

Figure 3. Biological functions of Hp. Hemolytic conditions, such as malaria, bacterial infection, sickle cell anemia, and severe injury induce red blood cell (RBC) lysis. Released free hemoglobin (Hb) from dead RBC is rapidly captured by Haptoglobin (Hp), and Hb-Hp complexes bind to the receptor CD163 that mediates a rapid endocytosis of the complexes on monocytes and macrophages. Hb-Hp complexes are degraded in lysosomes and this process is followed by heme releasing, and heme oxygenase (HO) catalyze conversion of heme fraction into biliverdin, carbon monoxide, and iron. Consequently, Hp prevents free Hb-induced inflammation and oxidative stress, and distributes restoration of iron by transport it to bone marrow.

I.4. Purpose of this study

It is well characterized that inflammation induces bone destruction by exerting RANKL expression in osteoblast to generate osteoclast formation. In line with RANKL induction, it has been reported that stimulation of inflammatory cytokines induced haptoglobin secretion (Heinrich et al., 1990). From this previous report, it is hypothesized that secreted-Hp may affect osteoclast differentiation. The aim of this thesis is to conduct studies on defining the role of Hp in osteoclast differentiation from osteoclast precursor cells—macrophages and to identify regulation of cellular metabolism in osteoclastogenesis. This study will contribute to understand the fundamental role of Hp as a coupling factor for osteoblast and osteoclast in bone biology, which in turn permits pivotal role of Hp in bone homeostasis maintenance.

II. Materials and Methods

II.1. Animal experiments

All animal experiments were performed in accordance with the Animal Care Committee of the Institute of Laboratory Animal Resources of Seoul National University (Seoul, Korea). C57BL/6.Hp$^{-/-}$ (Hp KO) mice were kind gifts from Dr. Lee Ann Garrett-sinha (Huntoon et al., 2013). 8-weeks-old male WT or Hp$^{-/-}$ mice (n = 6 per group) were intraperitoneally injected with PBS or RANKL (1 mg/kg of body weight) for every day. After 4 times injection, the mice were euthanized and the femurs were flash-frozen in liquid nitrogen and stored at -80 ℃ for RNA extraction or fixed in 4% paraformaldehyde for micro-computed tomography (μCT) measurement. The femurs were analyzed by high-resolution μCT (SMX-90CT system; Shimadzu, Kyoto, Japan). Scanning images from μCT were reconstructed by VG Studio MAX 1.2.1 program (Volume Graphics, Heidelberg, Germany). Each three-dimensional images were analyzed to measure bone volume, cortical bone volume, trabecular number, and trabecular separation by use of the TRI/3D-VIE (RATOC System Engineering, Kyoto, Japan).

Hp-injected animal model was performed by administration of PBS or mHp (100 μg/head) in 8-weeks-old male (n = 6 per group). Injection was

intraperitoneally administrated every other day after starting day. The mice were euthanized on day 14, and analyzed by μCT as described above.

II.2. Histology

The samples from animal experiments were decalcified with 12% EDTA for 3 weeks and embedded in paraffin. After histological sagittal sections (5 μm thickness), femurs were stained with tartrate-resistant acid phosphatase (TRAP) solution by use of Leukocyte Acid Phosphatase Assay kit with manufacturer's instructions (Sigma-Aldrich) or with hematoxylin and eosin (H&E) solution (Sigma-Aldrich). Appeared osteoclasts by TRAP stain were measured by use of OsteoMeasure XP program (version 1.01;OsteoMetrics, Decatur, GA, USA).

II.3. Reagents and antibodies

Recombinant human M-CSF, RANKL, bone morphogenetic protein 2 (BMP-2), mouse IL-1α, and LPS were obtained from PeproTech EC (London, UK). Plasma-derived human Hp and human Hb were purchased from Sigma-Aldrich (St. Louis, MO, USA). Mouse plasma-derived Hp was obtained from Lee Biosolutions (St. Louis, MO, USA). To detect target protein expression,

antibodies against NFATc1, c-Fos, and TLR4 were purchased from Santa Cruz Biotechnology, Inc (Santa Cruz, CA, USA). Antibodies against TLR4, FLAG and β-actin were purchased from Sigma-Aldrich. Secondary antibodies conjugated with horseradish peroxidase were obtained from Sigma-Aldrich. The specific neutralizing antibody against Toll-like receptor 4 (TLR4) was purchased from eBioscience (San Diego, CA, USA). The specific neutralizing antibody against IFN-β was purchased from PBL biomedical Laboratories (Piscataway, NJ, USA). The normal mouse IgG was purchased from Santa Cruz.

II.4. Cells and culture system

C57BL/6.TLR2-/-, C57BL/6.TLR4-/-, and C57BL/6.TLR7-/- mice were the kind gifts from professor Sungjoong Lee (Oh et al., 2011). Bone marrow cells were obtained by flushing bone marrow from femur and tibia of six-weeks-old male mice. The nonadherent bone marrow cells were further cultured with M-CSF (60 ng/ml) for 3 days with α-MEM to generate bone marrow-derived macrophages (BMMs) as described previously (Kim et al., 2013). To generate osteoclastogenesis, BMMs (4 X 10^4 cells/well) were cultured in 48-well plates with complete medium; α-MEM containing 10% heat inactivated fetal bovine serum (FBS) and 50 units/ml of penicillin in the presence of M-CSF (60 ng/ml)

and RANKL (100 ng/ml) for 4 days. The media was exchanged every 3 days. Appeared osteoclasts were washed with PBS, fixed with 3.7% formalin, and then stained for TRAP. Calvarial osteoblasts were isolated from calvariae of newborn mice as described previously (Lee et al., 2009). To generate osteogenic differentiation, osteoblasts were cultured in 48-well tissue culture plates precoated with collagen at a density of 5 X 10^4 cells/well. After culturing for 24 h, the cells were further cultured in osteogenic medium: α-MEM complete medium containing 10 mM β-glycerophosphate (Sigma Aldrich), 50μg/ml ascorbate-2-phosphate (Sigma Aldrich), and the 100 ng/ml of BMP-2 (PeproTech). The medium was replaced every 3 days. After culturing, the cells were fixed with 10% of formalin, then incubated with 0.1% Triton X-100 for 10 minutes. osteoblast differentiation was measured by alkaline phosphatase (ALP) or Alizarin Red S staining as manufacturer's instructions (Sigma-Aldrich).

The co-culture system was examined by culturing of BMMs (1 X 10^5 cells/well) and osteoblast (2 X 10^4 cells/well) with IL-1 (20 ng/ml) in 48-well tissue culture plates for 9 days. Appeared osteoclasts were stained by TRAP as described above.

II.5. ELISA

To analyze the secreted-Hp and secreted-IFN-β level, supernatant medium from cultured cell was harvested and centrifuged at 3000 rpm for 5 min to remove cell. Then, supernatant medium was recollected and measured by use of IFN-β ELISA kit (PBL) or Hp ELISA kit (Abnova, Taipei City, Taiwan) according to the manufacturer's instruction.

II.6. FITC-labeling and immunostaining

Fluorescein isothiocyanate (FITC) labeling of Hp was performed by using FluoroTag^{TM} FITC Conjugation kit (Sigma-Aldrich) according to manufacturer's instruction. BMMs were cultured in cover glasses plate in 12-well plate in the presence of M-CSF (60 ng/ml). After 24 h, Hp-FITC was added into cells, and incubated at 37°C for indicated time. The cells were washed with PBS for 2 times, and fixed with 3.7% formalin for 30 min. After blocking the cells with 1 % bovine serum albumin (BSA) in PBS for 30 min, antibody against TLR4 (2 μg) in 1 % BSA in PBS were added. After 1 h incubation on locker, the cells were washed with PBS for 3 times on the shaker. Then, anti-rabbit IgG antibody conjugated to Cy3 (Invitrogen) in 1 % BSA in PBS was added on cells and incubated for 30 min in dark room. The immunostained cells were observed under a confocal laser microscope

(Olympus FV-300, Tokyo, Japan).

II.7. Flow cytometry

BMMs (2 X 10^6 cells per dish) were cultured with M-CSF (60ng/ml) in 100 π culture dish. After 24 h incubation, the cells were treated with PBS, Hp (20 μg/ml) or LPS (1 μg/ml) for indicated time respectively. After incubation, the cells were detached by enzyme-free cell dissociation buffer (Millipore, Billerica, MA, USA). The cells were stained with anti-TLR4 antibodies, followed by FITC-conjugated anti-rat IgG, and analyzed by flow cytometry using a FACSCalibur (BD Biosciences, San Diego, CA, USA). Cells stained with isotype control antibodies were used as a negative control.

II.8. Cell viability assay

The cells (1 X 10^4) were cultured on 96-well culture plates. After 12 h incubation, the media was exchanged with PBS or the indicated doses of Hp. After indicated time of incubation, 10 μl of EZ-Cytox solution (Daeillab Service, Seoul, Korea) was added to each well of the plate. After incubation for 2h, the absorbance was measured by Multiskan (Thermo Labsystems,

Philadelphia, PA, USA) at 450 nm.

II.9. Western blot

To detect specific protein expression, the cells were lysed on ice with a buffer containing 20 mM Tris-HCl, 150 mM NaCl, 1% Triton X-100, protease inhibitor, and phosphatase inhibitor (Sigma Aldrich). After 30 min lysis in ice, the cellular debris was removed by centrifugation at 13,200 rpm for 15 min. The supernatant was collected in tube and protein concentration was determined by use of DC Protein Assay Kit (Bio-Rad, Hercules, CA, USA). The protein samples (20-50 μg) were separated by SDS-PAGE and electrotransferred onto polyvinylidene difluoride membrane (GE Healthcare, Chalfont St. Giles, Buckinghamshire, UK). The membrane was blocked with 5% skim milk, and target proteins were detected by indicated primary antibodies for overnight attaching. Attaching of secondary antibodies conjugated with horseradish peroxidase were used for blotting and were visualized by chemiluminescence reaction using ECL reagents (GE Healthcare).

II.10. Gene transduction and retroviral infection

Gene transduction was performed by use of Plat. E-retroviral packaging cells (Cell Biolabs, San Diego, CA, USA) according to the manufacturer's instruction. Retroviral vectors pMX-FLAG and pMX-constitutively active (CA)-c-Fos-FLAG, and pMX-constitutively active (CA)-NFATc1-FLAG were kindly provided by Dr. Nacksung Kim (Lee et al., 2009). The retroviral vectors were transiently transfected on Plat. E cell by using Genjet transfection reagent (SignaGen, Gaithersburg, MD, USA). After incubation for 48 h, supernatants containing retrovirus were collected. BMMs were then transduced with the retroviral supernatants in the presence of polybrene (6 μg/ml, Sigma-Aldrich) and M-CSF (60 ng/ml) for 12 h incubation. The cells were further cultured with puromycin (2 μg/ml) and M-CSF (60 ng/ml) for 3 days to remove uninfected cells.

II.11. Conventional and real-time PCR

To measure relative mRNA expression level, total RNA was isolated by use of TRIzol reagent (invitrogen). 2 μg of total RNA was used for first-strand cDNA synthesis by using SuperScript II Preamplification System (Invitrogen). For PCR amplification to target mRNA expression, 20 to 30 cycles were performed for each gene. PCR products were separated on a 1 to 1.2 % (v/v)

agarose gel, stained with ethidium bromide, and detected by ultraviolet light. The relative mRNA expressions were evaluated by ABI Prism 7500 sequence detection system with SYBR Green PCR Master Mix (Applied Biosystems, Foster City, CA, USA). Target mRNA expressions were determined according to the 2-ΔΔCT method using HPRT as a reference gene. Each primer set is shown in Table 1.

II.12. Hp-TLR4 binding assay

To identify the ability of Hp and TLR4 direct interaction, Hp-TLR4 binding assay was performed as described previously (Mossman et al., 2008). Briefly, high-binding immunoassay plate (Sigma-Aldrich) were coated with BSA, Hp or LPS with indicated dose for 24 h at 4°C, and the 2% BSA in PBS added to blocking for 1 h. After three washes with PBS containing 0.05% Tween 20, TLR4-Fc Fusion protein (2 μg) was added and incubated for 2 h in room temperature. The captured TLR4-Fc was detected by using a HRP-conjugated goat anti-human IgG Ab (Sigma-Aldrich), and then o-Phnylenediamine dihydrochloride (Sigma-Aldrich) was added to read spectrophotometrically at 450 nm by Multiskan (Thermo Labsystems).

II.13. Statistical analysis

All quantitative experiments were performed at least in triplicate. Student's t test was used to determine the tow-group comparisons significance. The *p*-values less than 0.05 were considered significant.

Real-time PCR primer sequences

Gene	Sequence		GenBank accession #
	Sense	Antisense	
	5'- -3'	5'- -3'	
RANKL	TGGAAGGCTCATGGTTGGAT	CATTGATGGTGAGGTGTGCA	NM_011613.3
OPG	TGGAACCCCAGAGCGAAACA	GCAGGAGGCCAAATGTGCTG	NM_008764.3
IFN-β	TGGGAGATGTCCTCAACTGC	CCAGGCGTAGCTGTTGTACT	NM_010510.1
IFN-γ	AGCAAGGCGAAAAAGGATGC	TCATTGAATGCTTGGCGCTG	NM_008337.4
NFATc1	CCGTTGCTTCCAGAAAATAACA	TGTGGGATGTGAACTCGGAA	NM_016791.4
c-Fos	ACTTCTTGTTTCCGGC	AGCTTCAGGGTAGGTG	NM_010234.2
c-Fms	TCTTCCTCTGTTCCCTTTCAGG	AGTTCTGTGAGGACGGGAAC	NM_001037859.2
RANK	TTCGACTGGTTCACTGCTCC	CTGTCGTTCTCCCCCACTTC	NM_006529381.2
IFNAR1	CAAGTGTGCCTGGCTTGTTC	GTGTACGACAGGCTCTTGCT	NM_010508.2
IFNAR2	AGAGCAACCCTTTCTCTGCC	GCCAACTCCCAGCAATTATGC	NM_010509.2
HO-1	CCTCACAGATGGCGTCACTT	GCTGATCTGGGGTTTCCCTC	NM_010442.2
HO-2	GTACAGAGAGAGTCGCAGACG	AGTAGTTTGTGCTGCCCTCA	NM_001136066.2
β-actin	CACTGTCGAGTCGCGTCC	CGCAGCGATATCGTCATCCA	NM_007393.5

Conventional PCR primer sequences

Gene	Sequence		GenBank accession #
	Sense	Antisense	

	5'- -3'	5'- -3'	
Hp	TCTGGGGTCAGCTTTTTGCT	AGCTGCCTTTGGCATCCAT	NM_017370.2
TLR2	AAGGAGGTGCGGACTGTTTC	AGTCAGGTGATGGATGTCGC	NM_011905.3
TLR4	CCCATGCATTTGGCCTTAGC	ACTCGGCACTTAGCACTGTC	NM_021297.3
TLR7	TGCACTCTTCGCAGCAACTA	TCACATGGGCCTCTGGGATA	NM_001290755.1
GAPDH	TGGAGAAACCTGCCAAGTATGAT	CCCTGTTGCTGTAGCCGTAT	NM_001289726.1

Table 1. PCR primers sequences used

III. Results

III.1. Protective effects of Hp on bone.

To understand the pivotal role of Hp in bone microenvironment, bones of 8-weeks-old wild-type (WT) or $Hp^{-/-}$ male mice were analyzed using micro-computed tomography (μCT) (n = 6 per group). Bone morphometric analyses revealed that the femurs from $Hp^{-/-}$ mice showed significantly lower bone volume and trabecula thickness, but increasing trabecular separation than that observed in WT mice (Fig. 4A and B). Histological analysis by H&E and TRAP staining further revealed that $Hp^{-/-}$ mice exhibited severe loss of bone with increased osteoclast formation (Fig. 5A and B). To determine whether RANKL induces Hp expression *in vivo*, soluble RANKL (200 μg per head) was injected intraperitoneally in 8-weeks-old male mice (n = 5 per group). Sera were collected from mice on day 0, 1, 2, and 3 after RANKL injection and serum Hp

levels determined. Serum Hp levels were markedly elevated on day 1 by RANKL injection, and were maintained until day 3 (Fig. 6). To further confirm the involvement of Hp level elevation in bone quantification, soluble RANKL (200 μg per head) was injected to WT or $Hp^{-/-}$ mice (Fig. 7). I observed that Hp deficiency significantly provoked RANKL-induced bone resorption in femurs, suggesting that Hp has a protective role against RANKL-induced bone destruction.

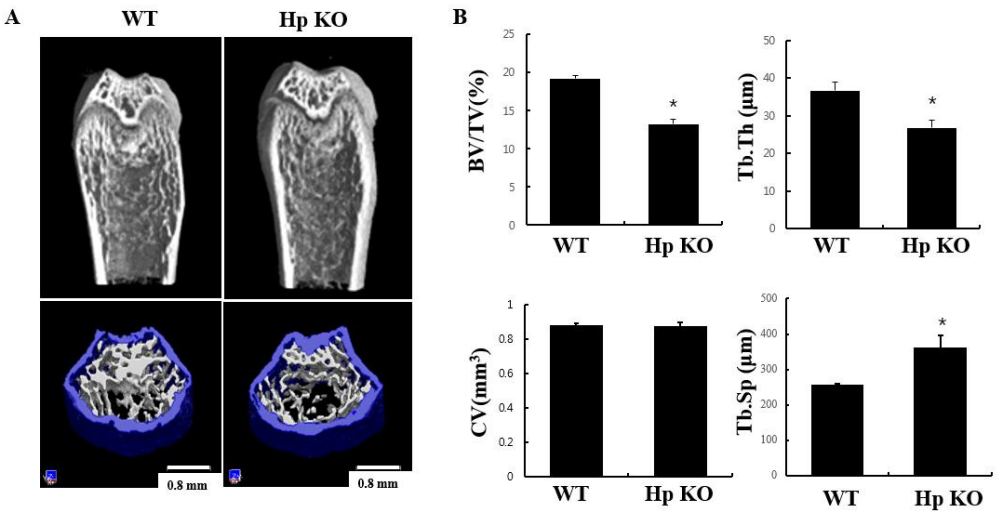

Figure 4. Hp KO mice showed decreasing of bone mass. The femurs of 8-weeks-old wild-type (WT) or $Hp^{-/-}$ (Hp KO) male mice were analyzed by μCT for bone mass (n = 6). (A) The images represent femurs (top) and its trabecular bones (bottom) of WT or Hp KO mice. Scale bar is 0.8 mm. (B) Reconstructed three-dimensional μCT images were analyzed for measuring bone mass. BV/TV, Bone volume/tissue volume; Tb.Th, trabecular thickness; Tb.N, trabecular number; Tb.Sp, trabecular separation. $^{*}p < 0.05$

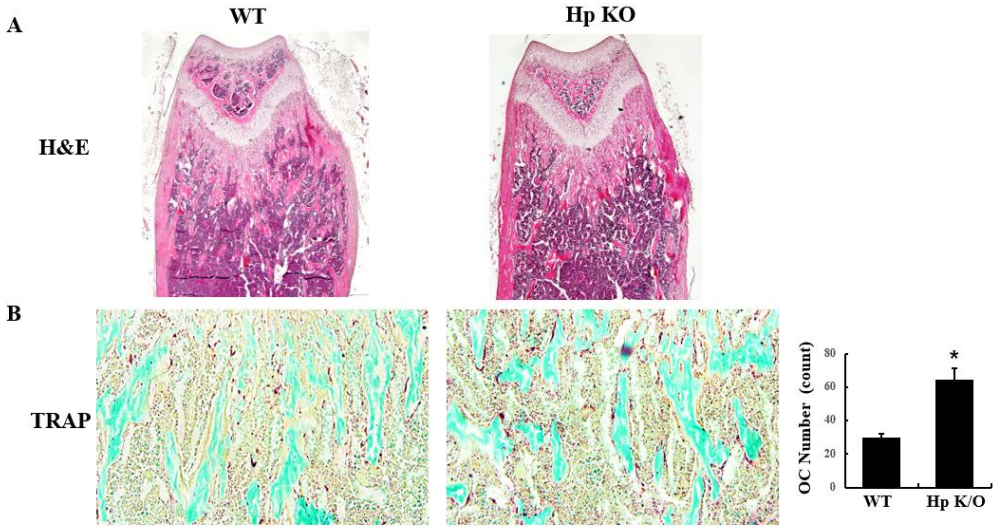

Figure 5. Hp KO mice have decreased bone mass with increasing osteoclast formation. (A and B) The femurs were investigated by histological sectioning and stained with H&E and TRAP, and TRAP-positive osteoclast number was counted. $^{*}p < 0.05$.

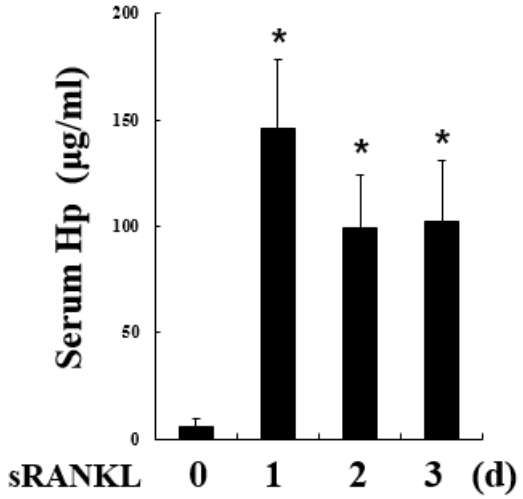

Figure 6. RANKL induced elevation of serum Hp. C57BL/6 mice (8-weeks-old, n = 5) were intraperitoneally injected with soluble RANKL (200 μg per head) for every day, and collected serums with indicated days were analyzed for secreted-HP level by using a mouse Hp-specific ELISA (*$P < 0.05$). d, day.

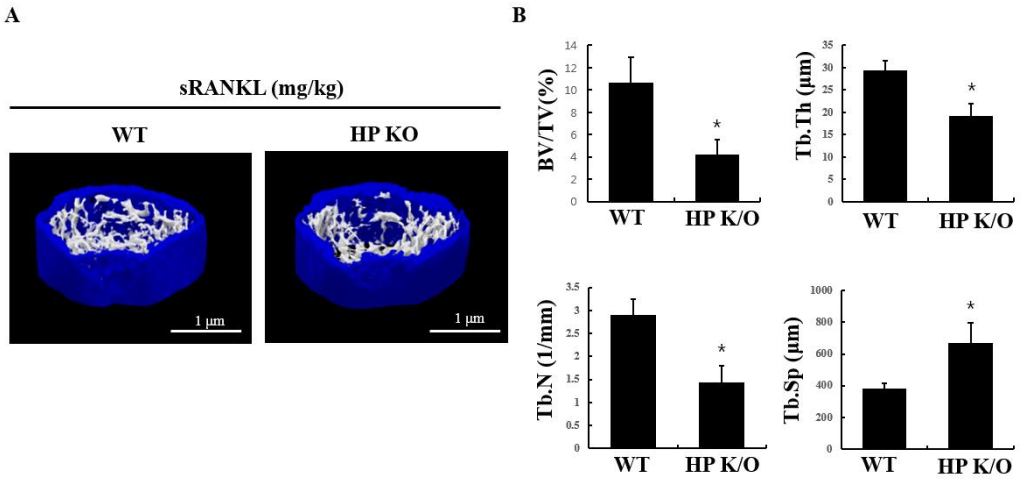

Figure 7. Deficiency of Hp induced severe bone loss in RANKL-injection model. The mice from WT or Hp KO (8-weeks-olds, n = 5) were intraperitoneally injected with soluble RANKL (1 mg/kg) for every day, and the femurs were dissected from mice on day 5 after first injection. Reconstructed three-dimensional μCT images were analyzed for measuring of quantitative bone. BV/TV, Bone volume/tissue volume; Tb.Th, trabecular thickness; Tb.N, trabecular number; Tb.Sp, trabecular separation. $^{*}p < 0.05$

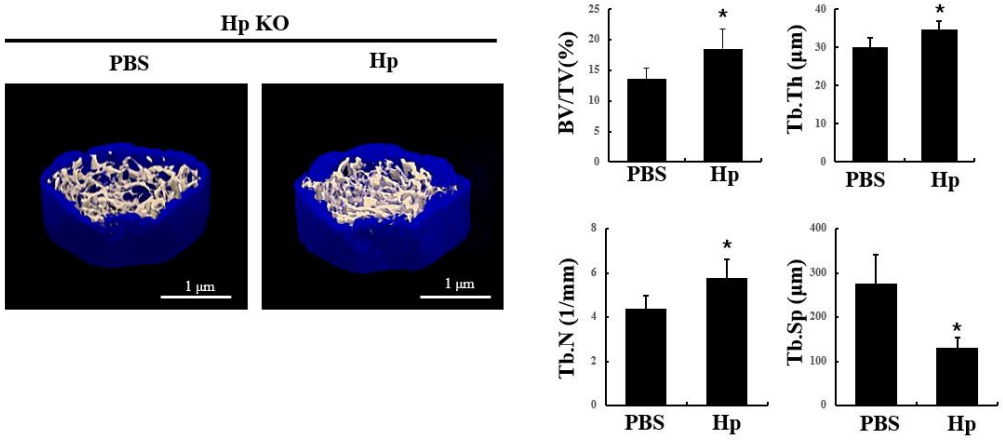

Figure 8. Administration of Hp increased bone volume in Hp KO mice. The mice from Hp KO (8-weeks-olds, n = 6) were daily injected intraperitoneally with mHp (1 mg/kg) for 7 days. The femurs were dissected from mice on day 8 and analyzed by μCT for measuring of quantitative bone. BV/TV, Bone volume/tissue volume; Tb.Th, trabecular thickness; Tb.N, trabecular number; Tb.Sp, trabecular separation. $^{*}p < 0.05$

III.2. The effects of endogenous Hp on osteoclastogenesis

In the previous results, I observed that absence of Hp showed bone loss phenotype with increasing osteoclast formation *in vivo*. These results raised the possibility that Hp might alter osteoclastogenesis directly by affecting osteoclast precursor cells to stimulate osteoclast differentiation. To investigate whether Hp regulates osteoclast differentiation, I thus primary cultured osteoclast precursor cells by extracting BMMs from WT or $Hp^{-/-}$ mice femur and tibia. In this study, I observed that RANKL-induced osteoclast differentiation was not affected by deletion of Hp (Fig. 8A). I next examined the effect of $Hp^{-/-}$ on key transcription factors for osteoclastogenesis, c-Fos and NFATc1, by western blotting. As shown in Fig. 8B, RANKL-stimulation induced an upregulation of c-Fos and NFATc1 expression during the osteoclast differentiation period, but no difference was shown between WT and $Hp^{-/-}$ BMMs. Indeed, expressions of Hp during M-CSF and RANKL induced-osteoclastogenesis were not detected in my culture system (data not shown). Collectively, these results indicated that endogenous expression of Hp did not affected RANKL-induced osteoclast differentiation.

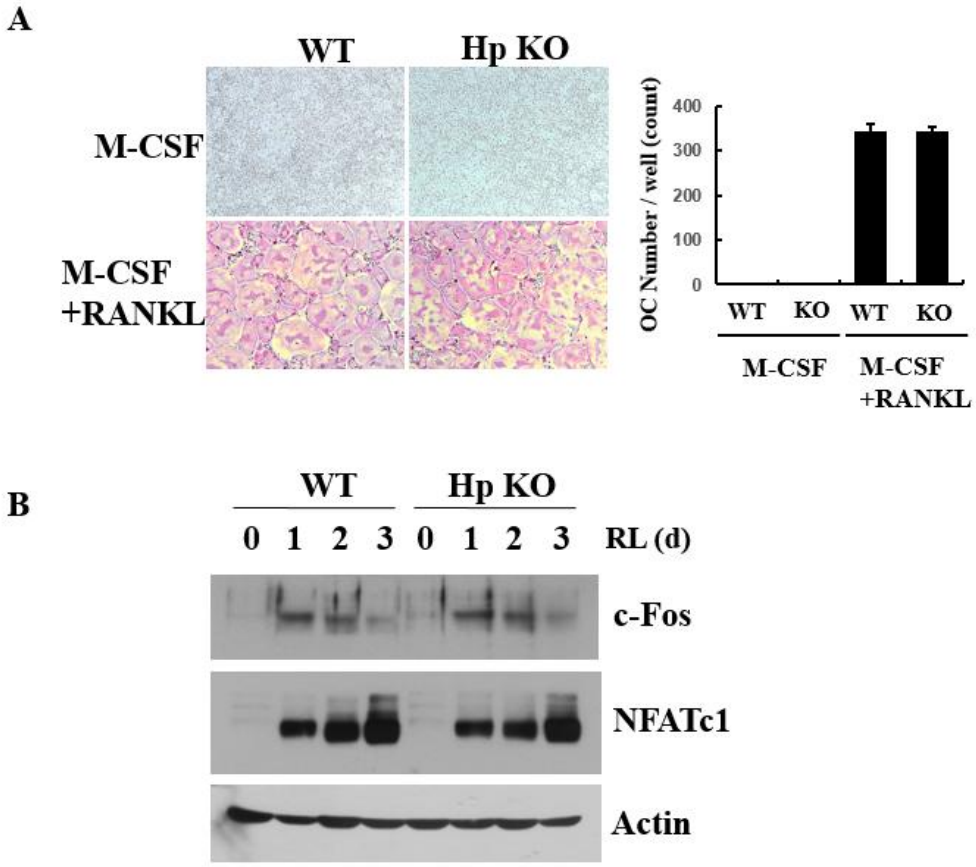

Figure 9. Deficiency of Hp did not affected on RANKL-induced osteoclastogenesis. Primary cultured BMMs from WT or Hp KO mice were induced osteoclast differentiation by stimulation of RANKL (100 ng/ml) in the presence of M-CSF (60 ng/ml) for 4 days. (A) Appeared osteoclasts were

stained for TRAP (left), and three or more nuclei-containing osteoclast were counted. (B) Culturing of BMMs in the indicated days were lysed and subjected to Western blotting with the specific antibodies. RL, RANKL; d, day.

III.3. Treatment of Hp inhibits osteoclast differentiation.

I next addressed the question of whether treatment with Hp affects osteoclast differentiation. To determine the effects of Hp on osteoclastogenesis, BMMs were cultured with PBS or various indicating doses of Hp in the presence of M-CSF and RANKL for 4 days. TRAP staining revealed that RANKL-induced osteoclast differentiation was gradually inhibited by increasing Hp dose (Fig. 9A and B). To further ascertain the biological potency of Hp against the survival of osteoclast precursor cells, BMMs were treated with various doses of Hp in the presence of M-CSF for the number of days indicated. As shown in Figure 9C, stimulation with Hp did not affected cells' survival during the M-CSF-induced cell growth period. These data suggested that Hp has inhibitory effects on RANKL-induced osteoclast differentiation without altering cells' survival. Osteoclastogenesis is a multiple step process that includes proliferation of osteoclast precursors, cell fusion, and osteoclast activation (maturation). To determine the precise step of osteoclast differentiation targeted by Hp, I treated BMMs with Hp at different time points during RANKL-induced osteoclastogenesis and analyzed osteoclast formation on day 4 using TRAP-

staining (Fig. 10). As shown in Figure 10A and B, simultaneous treatment of Hp with M-CSF and RANKL on the first day did not lead to effective osteoclast formation, whereas treatment with Hp on the second or on the third day after RANKL stimulation did not altered osteoclast formation. These results suggest that the inhibitory functions of Hp mainly affect the early stage of osteoclast differentiation.

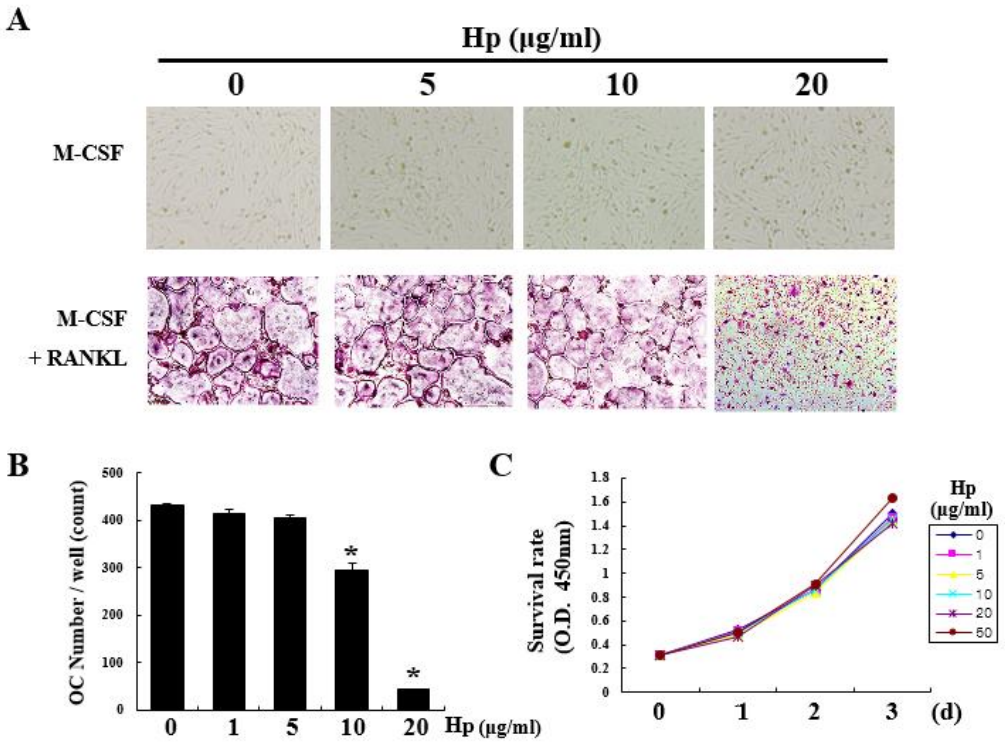

Figure 10. Hp treatment inhibits osteoclast differentiation. (A and B) BMMs were cultured with PBS or the indicated dose of Hp in the presence of M-CSF (60 ng/ml) and RANKL (100 ng/ml). After culturing for 4 days, (A) appeared osteoclasts were stained for TRAP, (B) and TRAP-positive three or more nuclei-containing osteoclasts were counted. $^{*}p < 0.05$. (C) BMMs were cultured with various doses of Hp in the M-CSF (60 ng/ml). After indicated days culturing, cell viability was measured. d, day.

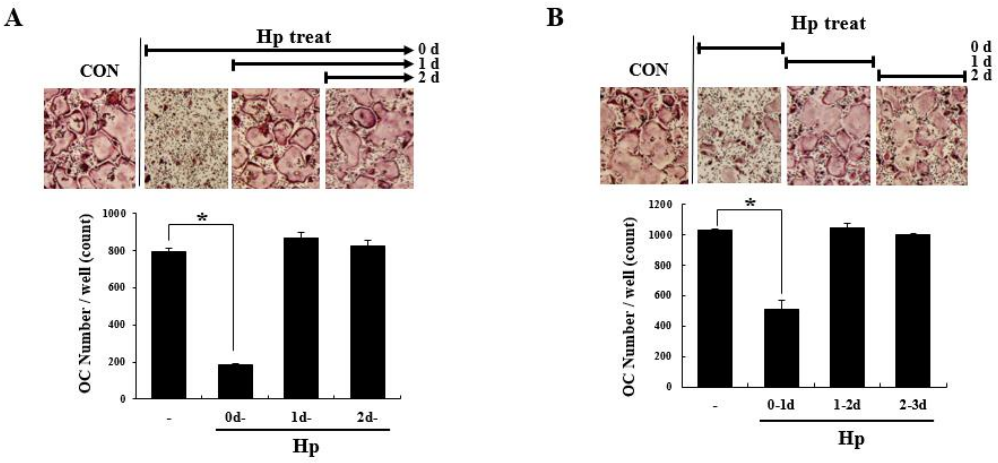

Figure 11. Treatment of Hp inhibits RANKL-induced osteoclast differentiation at early stage. (A and B) Hp was treated at indicated time periods during RANKL-induced osteoclastogenesis. After 4 days of culturing, the cells were fixed and stained for TRAP (top), and appeared TRAP-positive three or more nuclei-containing osteoclasts were counted (bottom). $^{*}p < 0.05$.

III.4. Hp inhibits RANKL-induced c-Fos expression

Since reduced-osteoclast number results in inhibitory effects on osteoclast differentiation, it is crucial to know how the extracellular stimuli lead to the activation of key transcription factor responsible for this process. To understand the molecular mechanism by which Hp regulates RANKL-induced osteoclast differentiation, I explored the effects of Hp on the expression of the key transcription factors, c-Fos and its downstream factor NFATc1 using western blotting. In the presence of M-CSF and PBS, stimulation of RANKL stimulation induced the upregulation of c-Fos and NFATc1 during the osteoclast differentiation period (Fig. 11). However, treatment with Hp significantly inhibited RANKL-induced c-Fos and NFATc1 protein expression. To further understand how the transcription factors were affected by Hp treatment, mRNA expression was analyzed using real-time PCR. mRNA expressions of the RANKL receptor RANK and M-CSF receptor c-Fms was not altered by Hp stimulation (Fig. 12). Interestingly, Hp stimulation did not affected c-Fos mRNA expression whereas its protein expression was completely blocked by Hp treatment. Furthermore, NFATc1, the downstream transcription factor of c-Fos, was considerably inhibited by Hp treatment. These results suggest that the inhibitory role of Hp might be mediated via the proteasomal degradation of c-Fos during RANKL-induced osteoclast differentiation.

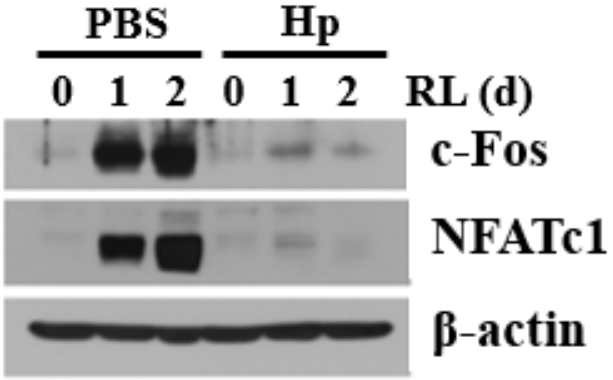

Figure 12. Treatment of Hp inhibited RANKL-induced c-Fos and NFATc1 expression. BMMs were cultured in the presence of M-CSF (60 ng/ml) alone or RANKL (RL; 100 ng/ml) together with PBS or Hp (20 μg/ml) for the indicated days. Total cell lysates were harvested and subjected to Western blotting with the indicated antibodies. d; day.

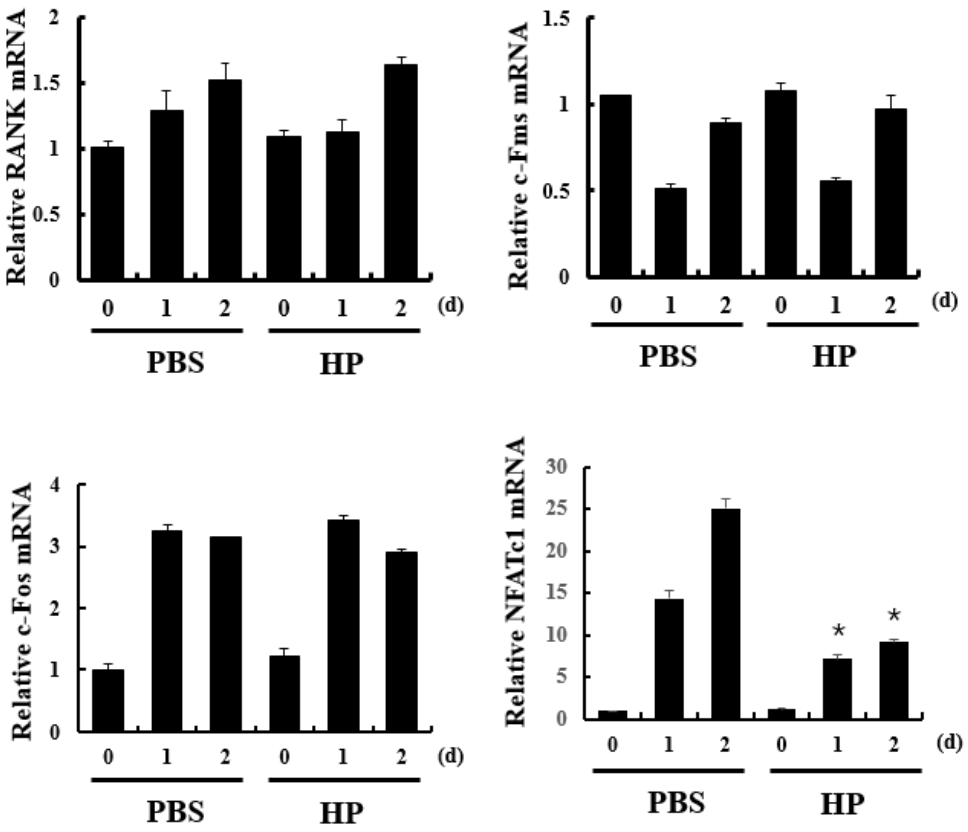

Figure 13. Hp did not affect mRNA expression of c-Fos. BMMs were cultured for the indicated times in the presence of M-CSF (60 ng/ml) alone or RANKL (RL; 100 ng/ml) together with stimulation of PBS or Hp (20 μg/ml). Total RNA was isolated, and the mRNA expression of RANK, c-Fms, c-Fos and NFATc1 were analyzed by real-time PCR with β-actin mRNA as an endogenous control. $^{*}p < 0.05$.

III.5. Hp inhibits c-Fos-dependent osteoclastogenesis

Previous results showed that treatment with Hp significantly suppressed osteoclast differentiation through downregulation of c-Fos and NFATc1 expression. To investigate whether the reduction in c-Fos and NFATc1 expression is mediated by an Hp-induced anti-osteoclastogenic effect, BMMs were overexpressed with pMX-IRES-FLAG-empty (Empty) or pMX-IRES-FLAG-constitutively active form of c-Fos (CA-c-Fos) and constitutively active form of NFATc1 (CA-NFATc1) using a retroviral infection system (Fig. 13A). In this study, the Hp-induced inhibitory effect in osteoclast differentiation was fully reversed by the forced expression of CA-c-Fos or CA-NFATc1 (Fig. 13B and C). As c-Fos upregulates its downstream transcription factor NFATc1 expression, I next explored whether the overexpression of CA-c-Fos affects NFATc1 expression. As shown in Figure 14, forced expression of CA-c-Fos recovered NFATc1 expression in the presence of Hp treatment. These results suggest that Hp exerts its anti-osteoclastogenesis effects through the inhibition of c-Fos expression.

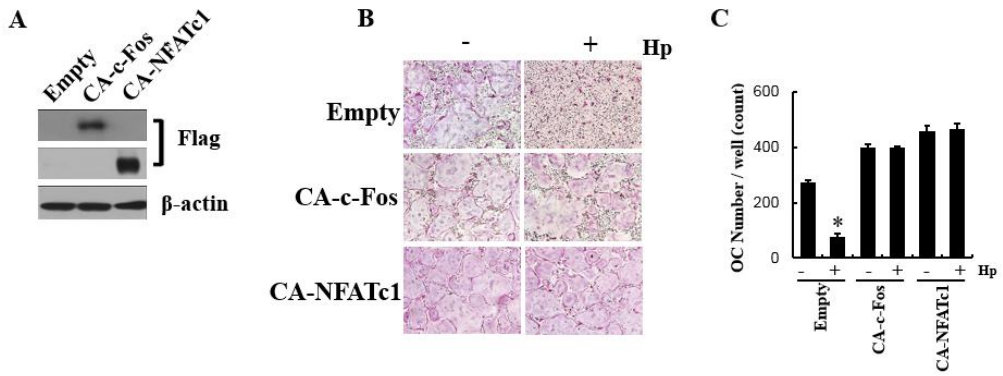

Figure 14. Overexpression of CA-c-Fos or CA-NFATc1 abolished the inhibitory effect of Hp in osteoclastogenesis. (A-C) BMMs were transduced with pMX-FLAG-empty (Empty) or pMX-FLAG-constitutively active form of c-Fos (CA-c-Fos) or pMX-FLAG-constitutively active form of NFATc1 (CA-NFATc1) respectively by retroviral infection. (A) The cell lysates from transduced BMMs were subjected to Western blotting. (B and C) The transduced BMMs were further cultured 4 days with PBS or Hp (20 μg/ml) in the presence of M-CSF (60 ng/ml) and RANKL (100 ng/ml) to generated osteoclasts. The appeared osteoclasts were then stained for TRAP, and TRAP-positive three or more nuclei-containing osteoclasts were counted. $^{*}p < 0.05$.

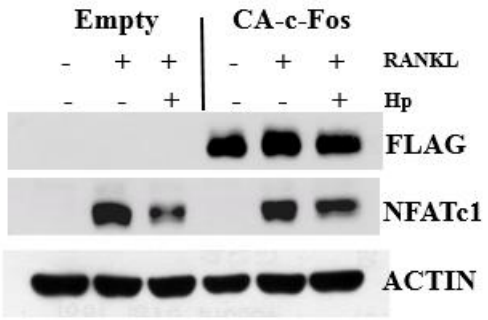

Figure 15. Hp-induced suppression of NFATc1 was recovered by overexpression of CA-c-Fos. The transduced BMMs with pMX-FLAG-empty (Empty) or pMX-FLAG-constitutively active form of c-Fos (CA-c-Fos) were further cultured with or without RANKL (100 ng/ml) and Hp (20 μg/ml) in the presence M-CSF (60 ng/ml). After culturing for 24 h, the cells were lysed and total cell lysates were subjected to Western blotting with the indicated antibodies.

III.6. Hp does not alter MAPKs and NF-κB signaling pathway

In the previous data, I observed that Hp-induced inhibitory effects against osteoclastogenesis is caused by suppression of c-Fos expression. These results led me to hypothesized that Hp may regulates upstream signaling of c-Fos. Previous studies revealed that RANKL-induced c-Fos expression is mediated by MAPKs and NF-κB signaling pathway (Boyce et al., 2015; Soysa et al., 2012). To find the mechanism of Hp-mediated regulation of c-Fos, I investigated the activation of MAPKs signaling pathways upon RANKL stimulation. RANKL-induced activation of ERK, JNK, and p38 were rapidly phosphorylated within 30 min (Fig. 15A). However, pre-treatment of Hp did not altered RANKL-induced activation of them. In addition, it is well known that AKT-mediated NFATc1 induction is independent of c-Fos during RANKL-induced osteoclast differentiation (Moon et al., 2012). As I expected, treatment of Hp did not affected RANKL-induced AKT phosphorylation (Fig. 15A).

Meanwhile, c-Fos expression also induced by canonical NF-κB signaling through RANKL-induced phosphorylation and degradation of Inhibitor of kappa B (IκB), which in turn permits releasing of P65/P50 heterodimers for translocation in nucleus and transcription its target genes (Boyce et al., 2015).

To ascertain whether Hp-induced suppression of c-fos is involved in NF-κB signaling, I investigated the activation of canonical NF-κB signaling during RANKL stimulation (Fig. 15B). However, treatment of Hp did not affect P65 and IκB phosphorylation when I compared to that of PBS treatment. These results suggest that Hp-induced suppression of c-Fos expression is not mediated by MAPKs, AKT, and canonical NF-κB signaling pathway.

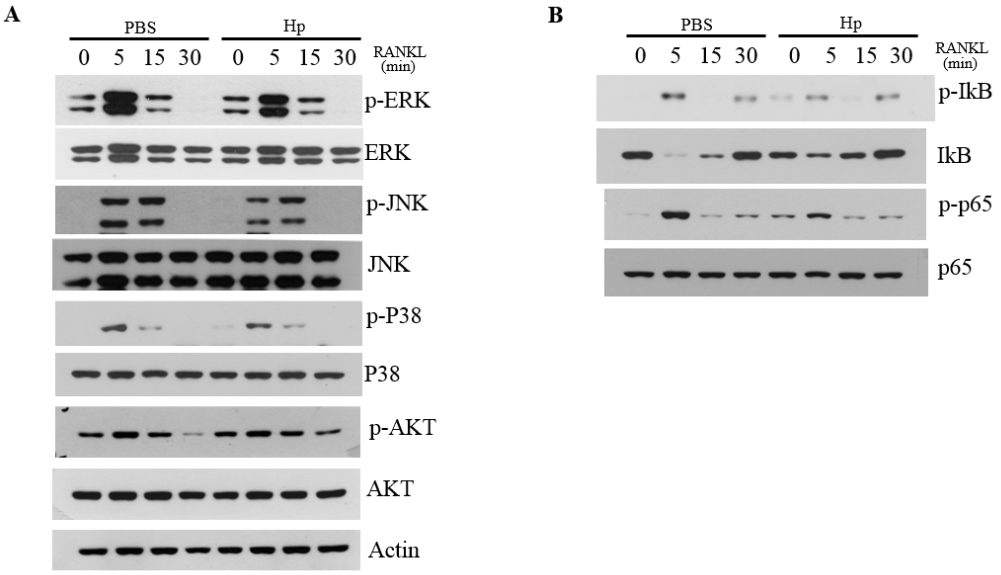

Figure 16. Treatment of Hp did not affect7 MAPKs, AKT, and canonical NF-κB signaling pathway. (A and B) BMMs were cultured for 24 h in the presence of M-CSF (60 ng/ml). After culturing, BMMs were serum- and cytokine-starved in the presence of PBS or Hp (20 μg/ml) for 1 h and then stimulated with RANKL (100 ng/ml) for the indicated time. Total cells were lysed and subjected to Western blotting to detect target proteins expression.

III.7. Hp induces IFNβ expression to inhibit c-Fos expression and osteoclastogenesis

During this study to identify the exact mechanism of regulation of c-Fos by Hp, I noted that the RANKL-induced MAPKs, AKT, and NF-κB signaling pathways were not involved and the evidence was insufficient to conclude that Hp-induction completely blocks c-Fos expression. Furthermore, mRNA expression of c-Fos was not altered by Hp stimulation. Thus, I speculated that Hp-induced suppression of c-Fos protein expression level might be due to proteasomal degradation. Indeed, it is well established that IFNβ has a remarkable inhibitory effect on osteoclastogenesis via selectively and dramatic downregulation of c-Fos protein expression (Takayanagi et al., 2002b). To ascertain whether the inhibitory action of Hp is mediated through IFNβ induction, mRNA expression of IFNβ and secreted-IFNβ were analyzed. As expected, Hp treatment resulted in significant elevation of IFNβ levels (Fig. 16A and B). However, IFNγ, also known as an osteoclastogenesis suppressor as it degrades TRAF-6, was not affected (Takayanagi et al., 2000). To address whether the Hp-mediated suppression of c-Fos was indeed caused by IFNβ, I next examined c-Fos expression recovery by using a IFNβ-specific neutralizing antibody. I observed that Hp-induced suppression of c-Fos and NFATc1 expression was substantially rescued by IFNβ neutralizing antibody (Fig. 17).

In line with this, I next investigated whether Hp induces IFNβ expression during RANKL-induced osteoclastogenesis. Although Hp-induced IFNβ mRNA expression was gradually decreased by RANKL-induced osteoclast differentiation, expression of IFNβ was higher than that observed following PBS treatment (Fig. 18). In addition, I found that blocking of IFNβ substantially suppressed the inhibitory effects of HP; however, it is still remained to have insufficient effects of IFNβ blocking to fully recover osteoclastogenesis (Fig. 19). Therefore, BMMs from WT or IFN receptor 1 knockout mice ($IFNAR1^{-/-}$) were isolated and differentiated into osteoclasts. Interestingly, the inhibitory effects of Hp against RANKL-induced osteoclastogenesis was fully abolished in $IFNAR^{-/-}$ BMMs (Fig. 20A). Furthermore, I found that treatment with Hp increased mRNA expression of IFNAR1 and IFNAR2 (Fig. 20B). These data suggested that Hp exerts its anti-differentiation effect through Hp-induced autonomous regulation of IFNβ.

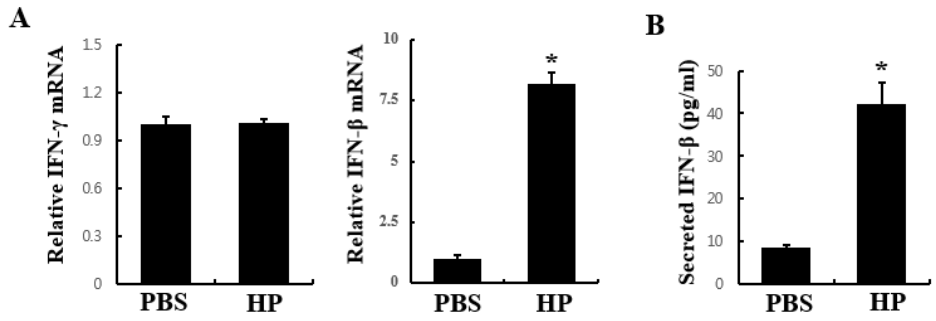

Figure 17. Hp induced IFNβ expression. (A and B) BMMs were cultured with PBS or Hp (20 μg/ml) in the presence of M-CSF (60 ng/ml). After culturing for 24 h, (A) total RNA was isolated and mRNA expression levels of IFNγ and IFNβ were analyzed by real-time PCR (left and middle). $^{*}p < 0.05$. (B) The secreted-IFNβ production from supernatant of BMMs were measured. $^{*}p < 0.05$.

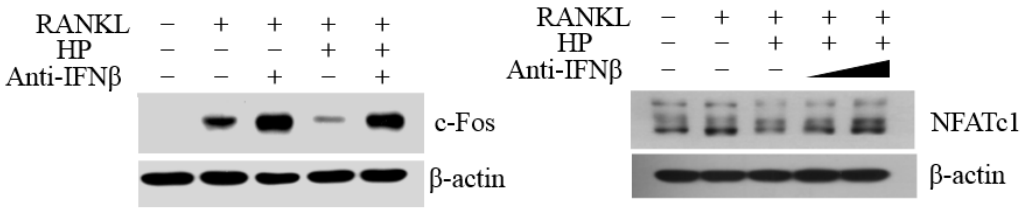

Figure 18. IFNβ blocking rescued Hp-induced suppression of c-Fos and NFATc1 expression. BMMs were cultured with indicated RANKL (100 ng/ml) and Hp (20 μg/ml) and specific-IFNβ neutralizing antibody (10 and 20 μg/ml) in the presence of M-CSF (60 ng/ml). After culturing for 24 h, the cells were lysed and total cell lysates were subjected to Western blotting with indicated antibodies.

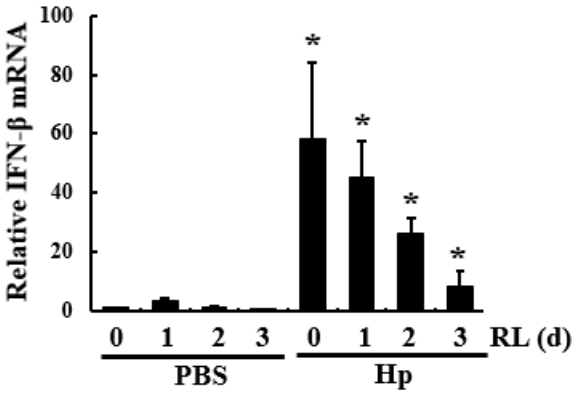

Figure 19. Hp induced IFNβ expression during RANKL-induced osteoclastogenesis. BMMs were cultured with PBS or Hp (20 μg/ml) in the presence of M-CSF (60 ng/ml) with or without RANKL (100 ng/ml). After culturing of indicated time, total RNA was isolated and analyzed mRNA expression by real-time PCR. $^{*}p < 0.05$. RL; RANKL, d; day.

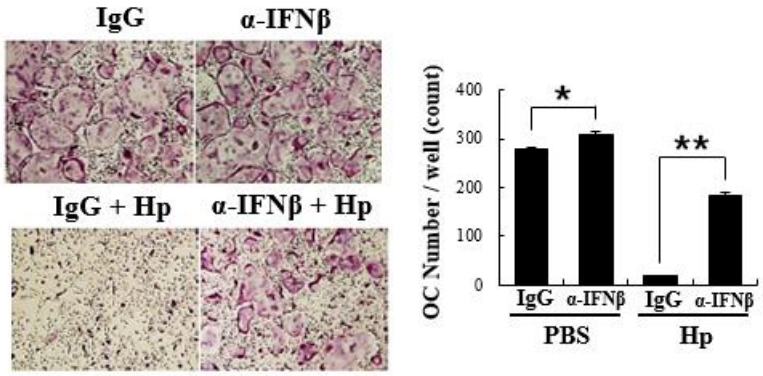

Figure 20. Blocking of IFNβ rescued inhibitory effects of Hp in osteoclast differentiation. BMMs were cultured with PBS or Hp (20 μg/ml) and irrelevant normal mouse IgG (10 μg/ml) or specific-IFNβ neutralizing antibody (10 μg/ml) in the presence of M-CSF (60 ng/ml) and RANKL (100 ng/ml). After culturing for 4 days, the cells were fixed and stained for TRAP (left). Appeared TRAP-positive osteoclasts that contained three or more nuclei were counted (right). $^{**}p < 0.01$, $^{*}p < 0.05$.

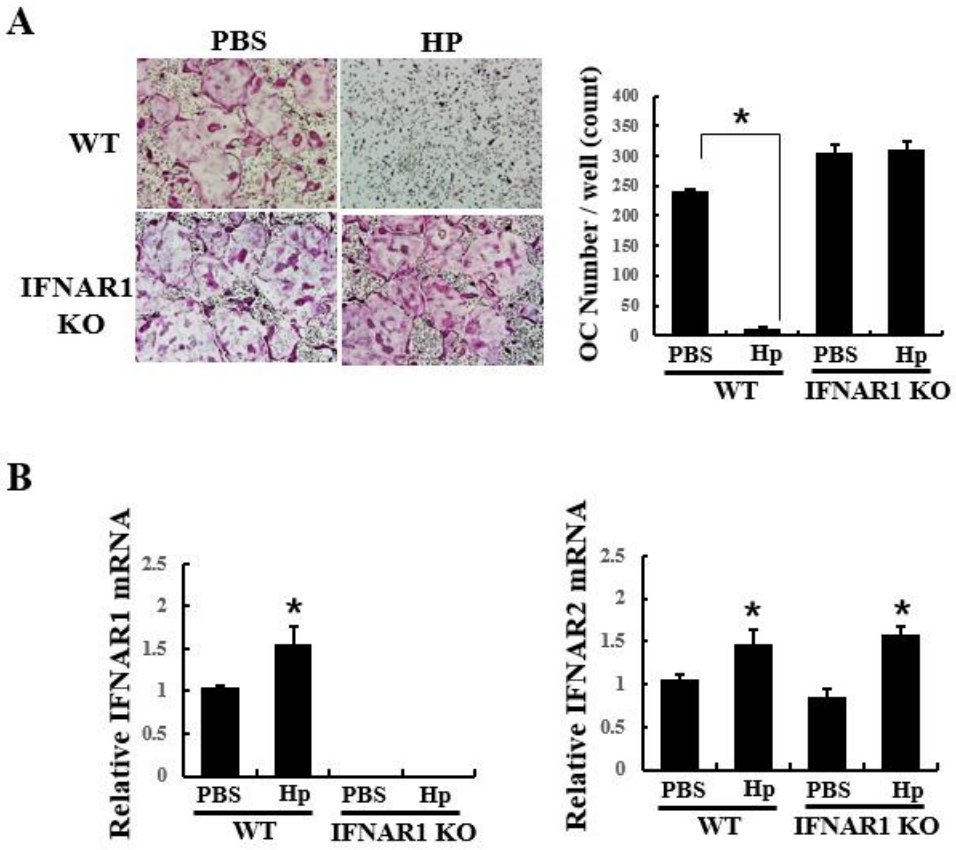

Figure 21. Inhibitory effects of Hp against osteoclastogenesis abolished in IFNAR KO BMMs. Isolated BMMs from WT or IFNAR KO mice's tibia were cultured for 24 h. (A) Total RNA was isolated and the expression levels of target mRNA were analyzed by RT-PCR. (B) WT or IFNAR KO BMMs were cultured with PBS or Hp (20 μg/ml) in the presence of M-CSF (60 ng/ml) and RANKL (100 ng/ml). After culturing for 4 days, the cells were fixed and

stained for TRAP. Appeared TRAP-positive cells containing three or more nuclei were counted (right). $^{*}p < 0.05$.

III.8. Induction of IFNβ is not mediated by Hb

Meanwhile, it is well established that biological function of Hp mainly attributes to interaction with Hb, then complexes of Hp-Hb bind to CD163 on macrophage for clearance of Hb-induced cell's cytotoxicity (Kristiansen et al., 2001; Tseng et al., 2004). In addition, there was no binding to CD163 detected in case of non-complexed Hb nor Hp alone. This raised the possibility that FBS containing Hb might be involved IFNβ expression through Hb-Hp complexes. Thus, I next examined the effect of Hp with Hb treatment on BMMs. Serum-free cultured BMMs showed increasing of IFNβ mRNA expression by Hp treatment, whereas treatment of Hb alone or Hb-Hp together reduced IFNβ (Fig 21A). Furthermore, Hb-Hp-CD163 complexes-induced mRNA expression of heme oxygenase 1 (HO-1) was not affected when I treated that with Hp alone (Fig 21B). These results suggest that Hp-induced IFNβ expression is not mediated by CD163 binding with Hp-Hb complexes.

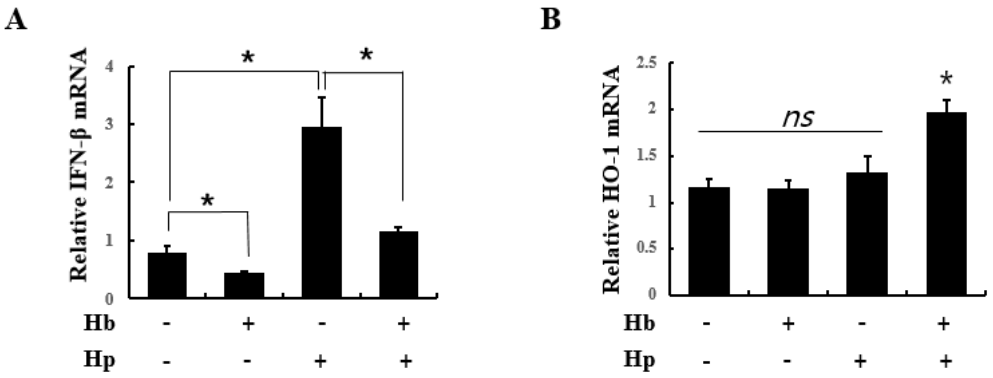

Figure 22. Hp-induced IFNβ expression was not mediated by Hb. (A and B) BMMs were cultured with M-CSF (60 ng/ml). After culturing for 24 h, the cells detached and exchanged with serum-free α-MEM with Hb (10 μg/ml) or Hp (20 μg/ml) or Hb and Hp together. The cells were further cultured for 24 h and total RNA isolated and mRNA expression levels of IFNβ and HO-1 were analyzed by real-time PCR. $^{*}p < 0.05$.

III.9. Hp induces IFNβ via TLR4

It is well established that induction of IFNβ is mediated through several Toll-like receptors (TLRs), including TLR2, 3, 4, 7, 8 and 9 (Aubry et al., 2012; Noppert et al., 2007). In order to identify Hp-binding receptor, I next explored whether several TLRs-KO BMMs, such as TLR2, TLR4, and TLR7 affect Hp-induced inhibitory effects on osteoclast differentiation. As shown in Figure 22A, deleted each gene, TLR2, TLR4, and TLR7 did not affected the other TLRs mRNA expression. Interestingly, TRAP-staining showed that inhibitory effects of Hp on osteoclastogenesis completely abolished on TLR4-deleted BMMs (Fig. 22B and C). Consistent with this results, I observed that induction of IFNβ mRNA expression by Hp was completely blocked on TLR4 knockout BMMs (Fig. 22D). To verify inhibitory effects of Hp on osteoclastogenesis due to the IFNβ, treatment of neutralizing antibody against IFNβ substantially rescued the Hp-induced suppression of osteoclastgenesis even on TLR2 or TLR7 KO BMMs (Fig. 23).

Since the IFNβ has a remarkable downregulation of c-Fos protein expression (Takayanagi et al., 2002b), I next investigated whether TLR4 was related to Hp-induced c-Fos suppression. As shown in Figure 24, Hp-induced suppression of

c-Fos and its downstream transcription factor NFATc1 were completely recovered in TLR4 KO BMMs. In addition to the effects of TLR4 deletion, blocking of TLR4 by its specific neutralizing antibody treatment also abolished Hp-induced suppression of osteoclastogenesis (Fig. 25). These results indicated that Hp suppresses osteoclastogenesis via TLR4-IFNβ signaling axis.

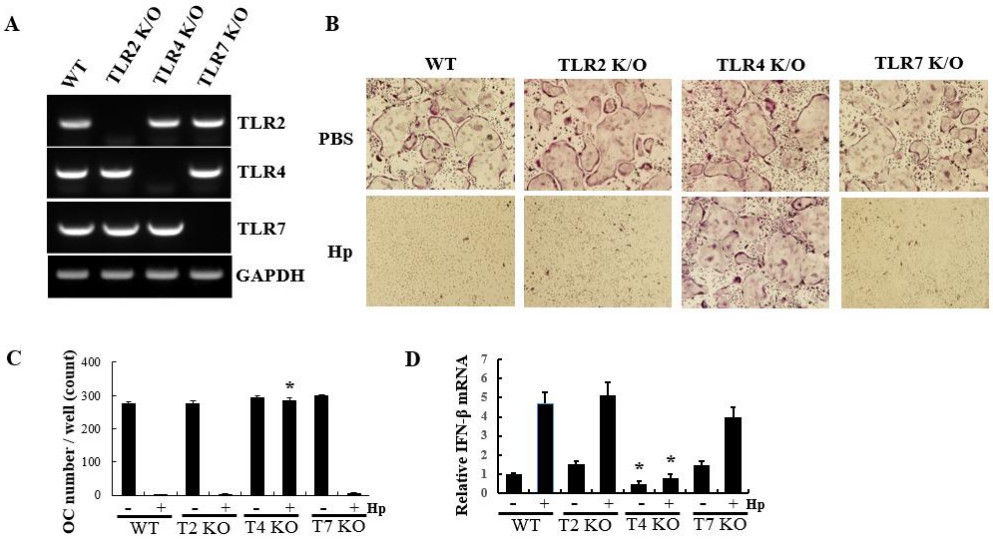

Figure 23. Inhibitory effects of Hp on osteoclastogenesis abolished on TLR4 KO BMMs. (A) Each BMMs, obtained from WT, TLR2 KO, TLR4 KO, and TLR7 KO mice were cultured for 24 h in the presence of M-CSF (60 ng/ml). After culturing, total RNA was isolated and mRNA expression levels of TLR2, TLR4, TLR7, and GAPDH were analyzed by conventional PCR. $^{*}p <$ 0.05. (B and C) The cells were cultured with PBS or Hp (20 μg/ml) in the presence of M-CSF (60 ng/ml) and RANKL (100 ng/ml) for 4 days. After culturing, the cells were fixed and stained for TRAP. (C) Appeared TRAP-positive cells containing three or more nuclei were counted $^{*}p < 0.05$. (D) Each BMMs cells were cultured with PBS or Hp (20 μg/ml) in the presence of M-

CSF (60 ng/ml) for 24 h. Then total RNA was isolated, and the expression of IFNβ mRNA was analyzed by real-time PCR with β-actin mRNA as an endogenous control. $^{*}p < 0.05$.

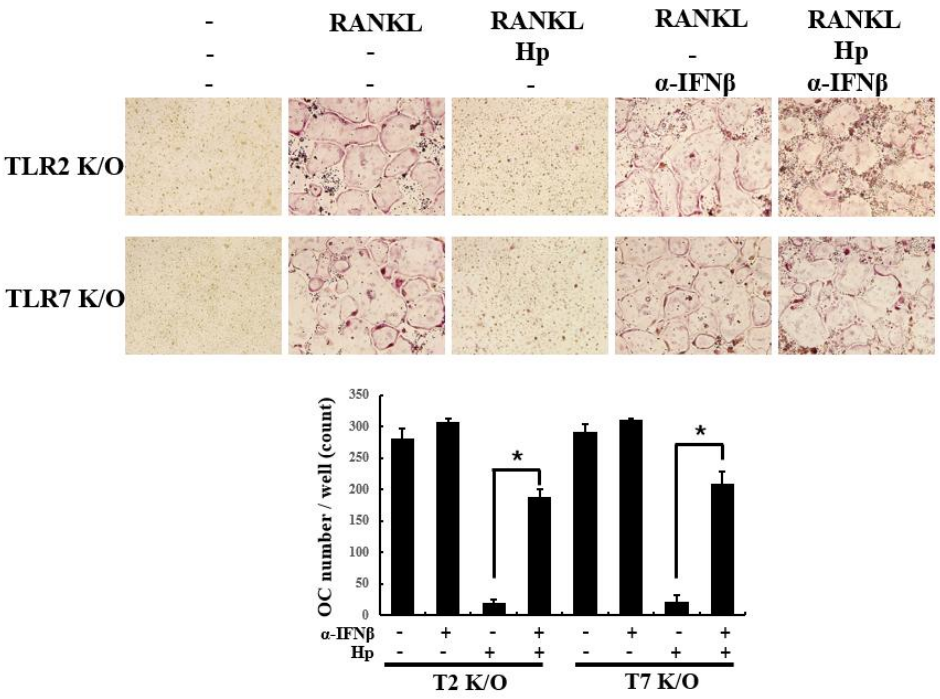

Figure 24. Inhibitory effect of Hp was abolished by IFNβ-neutralizing antibody on TLR2 KO or TLR7 KO BMMs. TLR2$^{-/-}$ or TLR7$^{-/-}$ BMMs were cultured with PBS or Hp (20 μg/ml), and irrelevant normal mouse IgG (10 μg/ml) or specific-IFNβ neutralizing antibody (10 μg/ml) in the presence of M-CSF (60 ng/ml) and RANKL (100 ng/ml). After culturing for 4 days, the cells were fixed and stained for TRAP, and the cells containing three or more nuclei

were counted. $^{*}p < 0.05$.

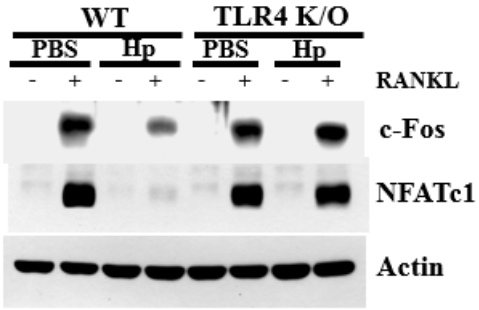

Figure 25. Hp did not affect c-Fos and NFATc1 expression in TLR4 KO cells. WT or TLR4 KO BMMs were cultured with PBS or Hp (20 μg/ml) with or without RANKL (100 ng/ml) in the presence of M-CSF (60 ng/ml). After culturing for 24 h, the cells were lysed and total cell lysates were subjected Western blotting with indicated antibodies.

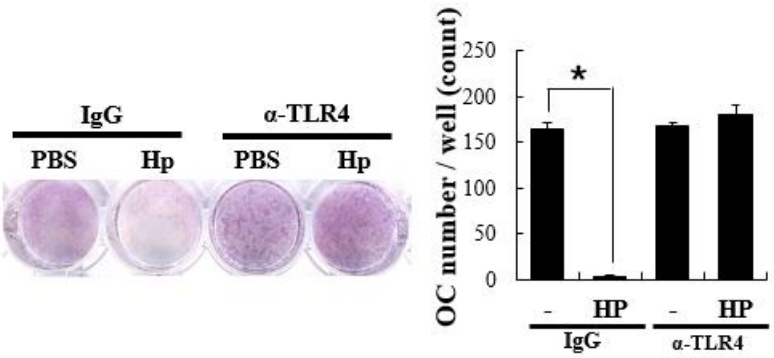

Figure 26. Blocking of TLR4 inhibited Hp-induced suppression of osteoclastogenesis. BMMs were cultured with PBS or Hp (20 μg/ml) and irrelevant normal mouse IgG (10 μg/ml) or specific-TLR4 neutralizing antibody (10 μg/ml) in the presence of M-CSF (60 ng/ml) and RANKL (100 ng/ml) for 4 days. After culturing for 4 days, the cells were fixed and stained for TRAP (left), and TRAP-positive cells containing three or more nuclei were counted (right). $^{*}p < 0.05$.

III.10. Hp directly binds to TLR4

Since I established that Hp negatively regulates osteoclastogenesis via TLR4, I next investigated whether Hp regulates TLR4 expression. Interestingly, Hp significantly downregulates TLR4 expression (Fig. 26A). In contrast, mRNA expression of TLR4 was elevated by treatment with Hp during RANKL-induced osteoclastogenesis (Fig. 26B). These results suggested that TLR4 might be involved in Hp-induced degradation. Indeed, it is well known that activation of the TLR4 by binding of ligands, such as LPS, initiates endocytosis of TLR4 with signal transduction, and leads to lysosomal degradation (Husebye et al., 2006; Noppert et al., 2007). Therefore, I proceeded to examine the identification of the Hp-induced molecular recognition events that determines the TLR4 expression in the plasma membrane. Incubation with LPS or Hp induced a gradual decrease in the level of TLR4 in the plasma membrane (Fig. 27). I also analyzed whether Hp and TLR4 colocalized in the plasma membrane at the early stages, i.e., before the internalization of Hp-TLR4 complexes. Analysis using confocal images of FITC-labelled Hp revealed colocalization with TLR4 within 60 min of treatment (Fig. 28). To determine whether Hp can directly bind to TLR4, I next performed a Hp-TLR4 binding assay using

recombinant TLR4 fused to the human Fc fragment of IgG1. As shown in figure 29, dose-dependent binding of immobilized Hp was observed, as LPS bound to TLR4 in a dose dependent manner. These observations suggest that Hp directly bind to TLR4 to induced intracellular signal transduction.

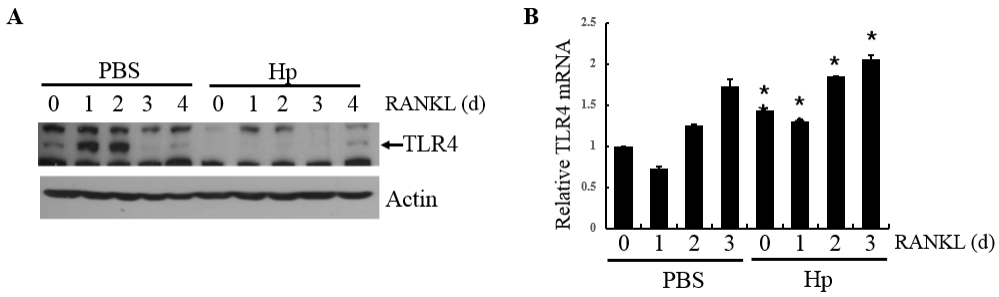

Figure 27. Hp suppressed TLR4 protein expression. (A and B) BMMs were cultured with PBS or Hp (20 μg/ml) with the M-CSF (60 ng/ml) alone or RANKL (100 ng/ml) together for indicated day. The samples were harvested and subjected to Western blotting or real-time PCR to measure TLR4 expression levels. $^{*}p < 0.05$.

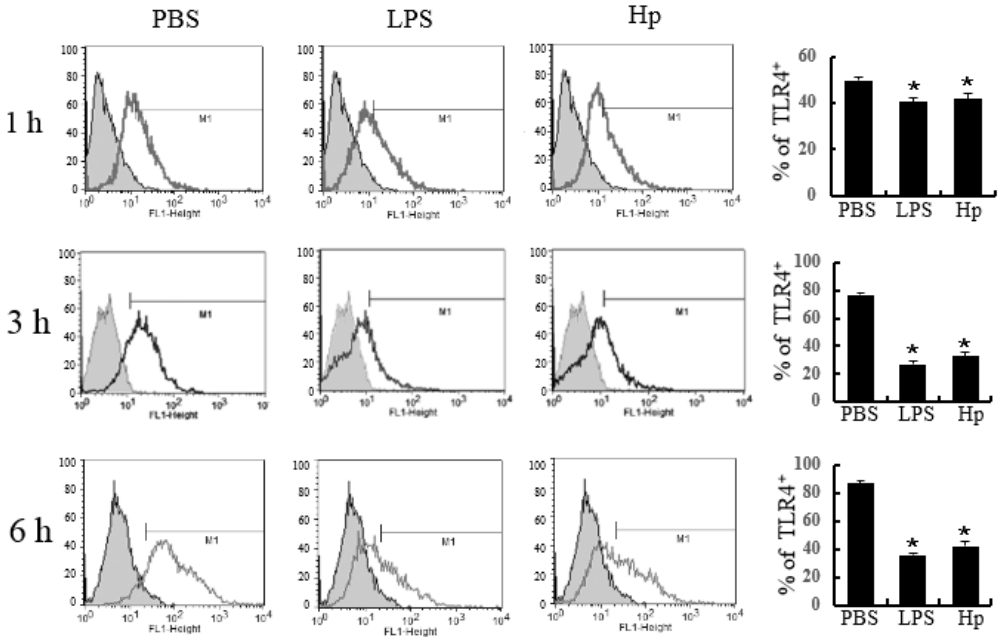

Figure 28. Hp induced TLR4 internalization. BMMs were cultured with M-CSF (60 ng/ml). After culturing for 24 h, the cells were incubated with PBS, Hp (20 μg/ml), and LPS (1 μg/ml) respectively. After incubation for indicated time, the cells were detached and analyzed cell surface-TLR4 by flow cytometry. $^{*}p < 0.05$.

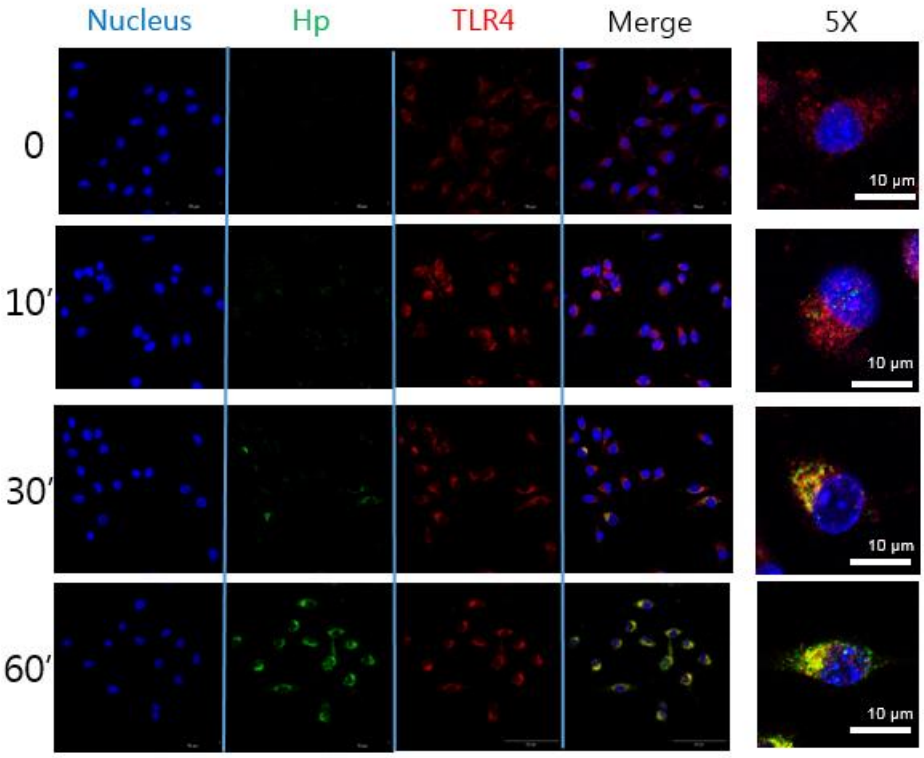

Figure 29. Hp colocalized with TLR4. BMMs were cultured in presence of M-CSF (60 ng/ml). After culturing for 24 h, the cells were incubated with Hp-FITC (green) for indicated times. The cells then fixed, and stained with TLR4 Ab (green) with DAPI staining for nuclei (blue).

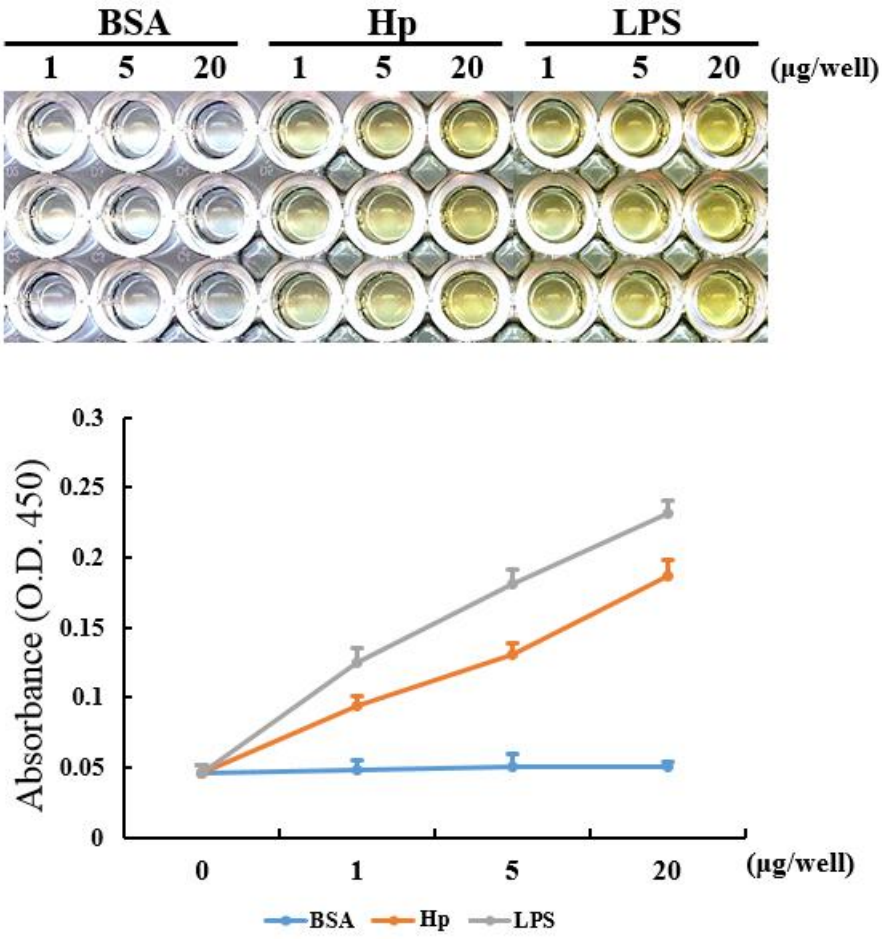

Figure 30. Hp directly binds to TLR4. High-binding immunoassay plate were coated with indicated dose of BSA, Hp, and LPS respectively. Immobilized each protein was then incubated with 2 μg of TLR4-Fc fusion protein. Binding ability with TLR4 was measured by HRP-conjugated anti-human IgG, then read spectrophotometrically at 450 nm.

III.11. The role of Hp in osteoblasts

In the bone environment, osteoclast differentiation is regulated by RANKL-expressing osteoblasts. Under pathological condition, several factors, such as IL-1α, IL-6, TNFα and LPS, have been shown to promote RANKL expression while decreasing its decoy receptor OPG in osteoblasts (Collin-Osdoby et al., 2001; Weitzmann, 2013). Thereby, this condition promotes osteoclast differentiation by coupling with RANKL-expressed osteoblasts. However, the role of Hp in osteoblast differentiation is poorly understood. Prior to the investigation of relationship between Hp and osteoblast-osteoclast coupling, I first examined the effects of Hp on osteoblast differentiation. ALP and alizarin red staining showed that treatment of Hp with various doses did not affected osteogenesis in calvarial osteoblasts (Fig. 30A). In addition, mRNA expression for ALP and OCN also was not affected by Hp (Fig. 30B). I next confirmed the effect of deletion of endogenous Hp in osteoblast differentiation. However, I observed that osteoblasts from $Hp^{-/-}$ mice did not affect not only in ALP and alizarin red staining, but also in ALP and OCN mRNA expression, from WT mice (Fig. 31A and B). I investigated the effects of Hp on IL-1α induced osteoclastogenesis by co-culturing with osteoblasts and BMMs. As expected, Hp-induced inhibitory effects were dose-dependent (Fig. 32A), whereas IFNβ mRNA expression was elevated (Fig. 32A). Indeed, I observed that osteoblasts

did not expressed IFNβ following Hp treatment (data not shown). These results indicated that Hp exerts inhibitory effects on IL-1α induced by indirect osteoclast differentiation via increasing of IFNβ in BMMs. However, Hp could reduce RANKL in IL-1α-treated osteoblasts. Thus, I next examined the effect of Hp on RANKL expression in osteoblasts. As shown in figure 33, IL-1α induced upregulation of RANKL whereas downregulation of OPG did not altered Hp treatment. Consistent with these results, I next checked the expression of Hp by stimulating various factors. Interestingly, several factors, including IL-1α, TNFα, and LPS induced Hp mRNA expression, partially effecting VD3, but not effect on BMP-2 (Fig. 34A). Furthermore, the amount of secreted Hp was increased in the cultured supernatants of osteoblasts in the presence of IL-1α or TNFα (Fig. 34B). These results raised the possibility that inflammatory factors-induced Hp production from osteoblasts may have a negative effect on osteoclastogenesis. To determine whether osteoclast differentiation was regulated by IL-1α-induced Hp expression in osteoblasts, I co-cultured WT or $Hp^{-/-}$ osteoblasts with BMMs. Importantly, IL-1α-induced osteoclast formation was significantly higher in $Hp^{-/-}$ osteoblasts than in WT osteoblasts (Fig. 35A). Similarly, the IL-1α-induced RANKL/OPG ratio was not altered in $Hp^{-/-}$ osteoblasts, whereas IFNβ was significantly downregulated in $Hp^{-/-}$ osteoblast. Collectively, these results indicated that secreted-Hp from osteoblasts

negatively regulates osteoclastogenesis to inhibit excessive osteoclast formation.

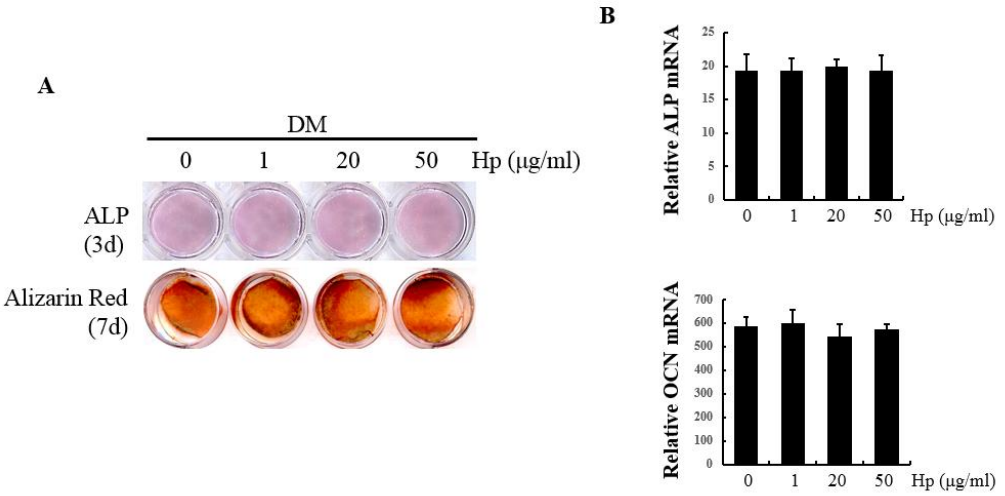

Figure 31. Treatment of Hp did not affect osteogenesis. (A and B) Calvarial osteoblasts were cultured in osteogenic media containing 10 mM β-glycerophosphate, 50μg/ml ascorbate-2-phosphate, and the 100 ng/ml of BMP-2 with indicated dose of Hp. (A) After culturing for 3 days, the cells were stained for ALP (top). Alizarin Red S staining was performed on day 9 (bottom). (B) After treatment of osteogenic media, mRNA expression for ALP or OCN were analyzed on day 3 or 7 respectively.

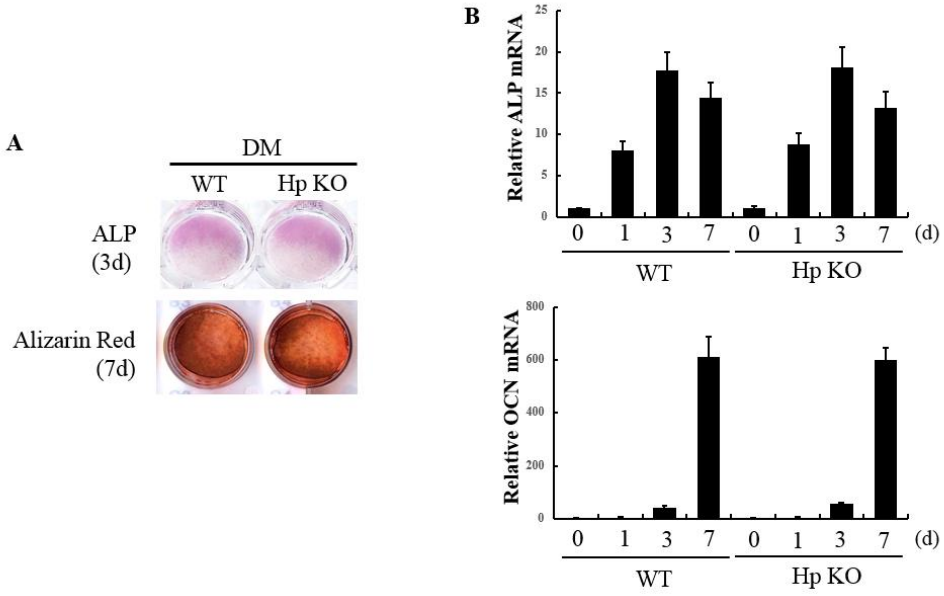

Figure 32. Deletion of Hp did not affect osteogenesis. (A and B) Calvarial osteoblasts were isolated from WT of Hp KO new born mice. (A) After culturing the cells with osteogenic media for 3 days, ALP staining was performed (top). Further cultured osteoblast with osteogenic media were stained for Alizarin Red S on day 9 (bottom). (B) After treatment of osteogenic media, mRNA expression for ALP or OCN were analyzed on day 0, 1, 3, and 7 by real-time PCR.

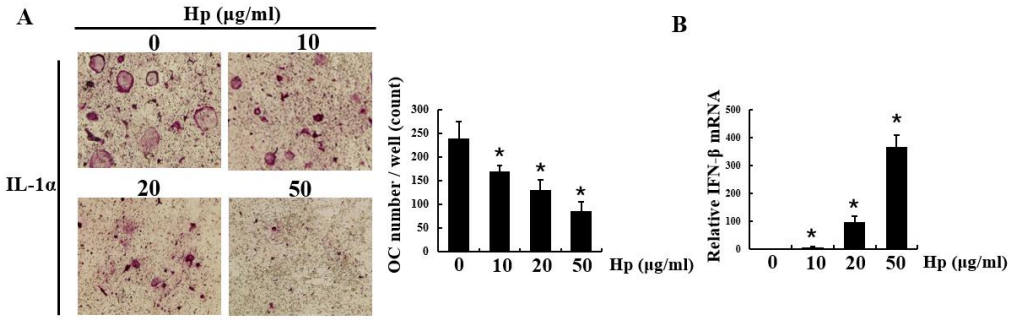

Figure 33. Hp inhibited osteoclastogenesis in co-culture system. (A and B) The co-culture of BMMs and osteoblast was performed in the presence of IL-1α (20 ng/ml) for 9 days. Appeared osteoclasts were stained for TRAP (A) or RNA was isolated from total cells to measure IFNβ mRNA expression. $^{*}p < 0.05$.

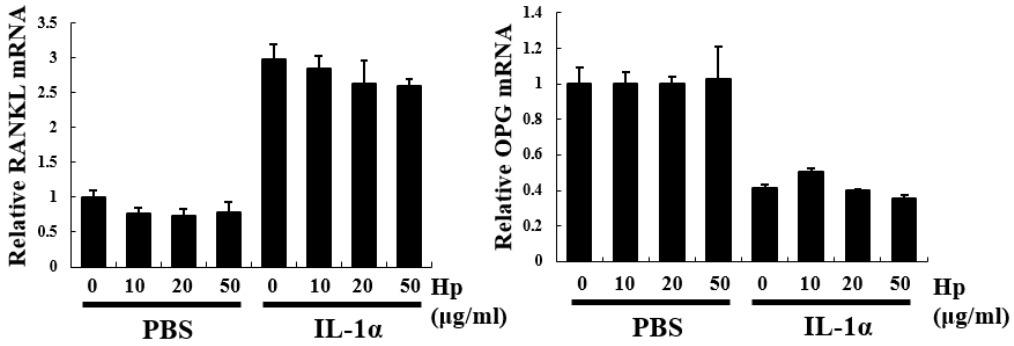

Figure 34. Stimulation of Hp did not affect IL-1α -induced RANKL and OPG expression. Osteoblasts were cultured with indicated dose of Hp in the presence of PBS or IL-1**α** (20 ng/ml) for 24 h. After culturing, total RNA was isolated and analyzed mRNA expression for RANKL and OPG by real-time PCR.

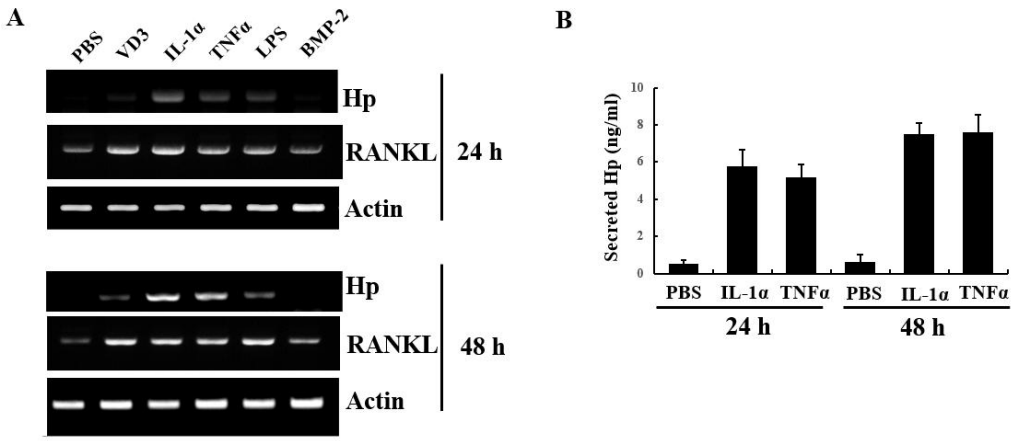

Figure 35. Inflammatory cytokines induced Hp secretion in osteoblast. (A and B) Osteoblasts were cultured with treatment of PBS, VD3 (10 nM), IL-1α (10 ng/ml), TNFα (10 ng/ml), LPS (10 ng/ml), and BMP2 (100 ng/ml) respectively. (A) After culturing for 24 h or 48 h, total RNA was extracted and analyzed mRNA expression with indicated specific primers. (B) After culturing for 24 h or 48 h, supernatant medium was collected and measured secreted Hp by use of ELISA.

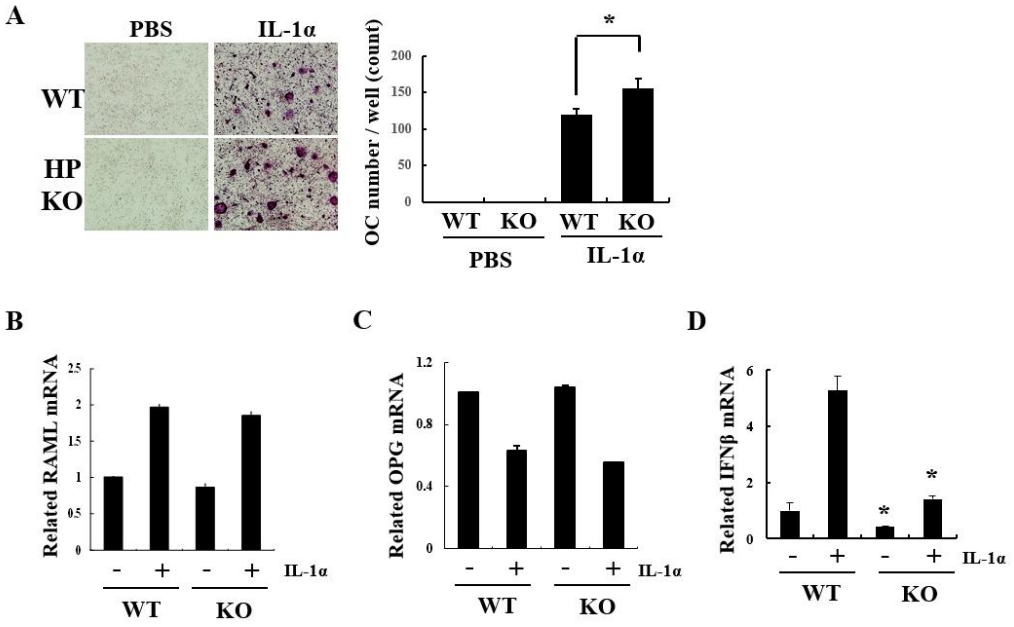

Figure 36. Absence of Hp provoked excessive osteoclast formation. (A) WT or Hp KO osteoblasts were cocultured with BMMs in the presence of PBS or IL-1α (20 ng/ml) for 9 days. After culturing, the cells were fixed and stained for TRAP to measure osteoclast number (left). And TRAP-positive cells containing three or more nuclei were counted (right). (B, C, and D) WT or Hp KO osteoblasts were cocultured with BMMs in the presence of PBS or IL-1α (20 ng/ml) for 1 days. Total RNA was extracted and analyzed mRNA expression for RANKL, OPG, and IFNβ by use of real-time PCR. $^{*}p < 0.05$.

IV. Discussion

Hp was initially identified as one of the acute phase plasma proteins that interacts with Hb. Therefore, evidence has accumulated for a role of Hp binding with extracellular Hb, allowing detoxification of Hb-mediated tissues damage, including vascular, liver, kidney, and spleen damage (Schaer et al., 2013). Understandably, it is apparent that Hp is capable of blocking the action of Hb-induced tissues damages; however, I focused on Hp-mediated intracellular signaling during RANKL-induced Osteoclastogenesis and its key role in bone protection properties.

In the RANKL-administration animal model, I observed a simultaneously increasing levels of serum Hp and bone destruction (Fig. 6 and 7). This phenomenon raised the possibility that RANKL-induced elevation of Hp may contributes to bone destruction. However, $Hp^{-/-}$ mice showed severe bone loss, whereas administration of Hp increased bone volume (Fig. 4 and 8). Insight into the physiological actions of Hp suggested that Hp participates to compensate in RANKL-induced excessive osteoclast formation, and leads to bone destruction. Importantly, previous reports showed that reduced bone mass density is associated with hemolysis in patients with sickle cell diseases (Baldanzi et al., 2011). Indeed, it is well-known that oxidative stress-ROS, and intravascular

hemolysis activation over its clearance provoked sickle cell disease (Schaer et al., 2013). Therefore, I speculated that Hp might be involved in indirect regulation of osteoclast differentiation by Hb-induced ROS production blocking, and this proposal was supported by previous reports that ROS stimulates RANKL-induced osteoclast differentiation (Ha et al., 2004; Lee et al., 2005). However, I observed that the treatment of Hp directly reduced osteoclast differentiation at early stage (Fig. 10), but not in the late stage. This observation suggested that stimulation of Hp induces immune events in BMMs rather than in RANKL-induced osteoclast differentiation. Similarly, it is well-known that LPS inhibits osteoclast differentiation by TLR4 receptor stimulation, consequently activating immune responses to prevent pathogenic effects (Takami et al., 2002; Zou and Bar-Shavit, 2002). In contrast, LPS induces osteoclast differentiation indirectly in an osteoblast co-culture system by stimulating RANKL expression in osteoblast (Sato et al., 2004). Therefore, LPS has been used predominantly to induce osteoporosis in animal models (Hussain Mian et al., 2008; Orcel et al., 1993; Sakuma et al., 2000). Importantly, I observed that treatment with Hp did not alter RANKL expression in osteoblasts (Fig. 33). In addition, Hp inhibited IL-1α- induced osteoclast differentiation in co-culture system without changing the level of RANKL and OPG expression (Fig. 35). Although LPS-induced RANKL expression is mediated via TLR4-

MyD88 signaling axis in osteoblasts (Sato et al., 2004), I suggested that Hp-mediated receptor activation in osteoblast is ineffective or modulated by another unknown receptor.

It is well established that inflammatory factors, IL-1 and IL-6 stimulate Haptoglobin production in hepatocyte (Prowse and Baumann, 1989). Recent studies also revealed that inflammatory cytokines upregulate Hp mRNA expression in mature adipocytes (do Nascimento et al., 2004; Friedrichs et al., 1995), and keratinocyte cell line HaCaT (Xia et al., 2008). In this study, I observed that stimulation of inflammatory cytokines, such as IL-1α and TNFα significantly induce Hp expression in osteoblasts (Fig. 34). Although deletion of or treatment with Hp did not affected osteogenesis (Fig. 30 and 31), these results indicated that osteoblasts that originated from mesenchymal stem cells (MSCs) participate in immune response indirectly through the secretion of Hp and in turn IFNβ production in BMMs. Previous studies have reported that expression of IFNβ is expressed in response to the several TLRs activation, including TLR2, 3, 4, 7, 8 and 9 in macrophages (Aubry et al., 2012; Noppert et al., 2007). In this study, I found that deletion of TLR4 abolished Hp-induced IFNβ expression (Fig. 22). Indeed, IFNβ is one of the type I IFNs, effectively expressed at local sites in an autocrine manner via its receptor IFNAR (Noppert et al., 2007). In agreement with the previous finding, I first observed that Hp

treatment during RANKL-induced osteoclastogenesis showed significant induction of IFNβ expression (Fig. 18). Furthermore, treatment with IFNβ neutralizing antibody or deletion of IFNβ receptor showed substantially abrogation of inhibitory effects of Hp in osteoclastogenesis (Fig. 19). These results indicate that secreted IFNβ regulates osteoclastogenesis in an autonomous manner. Interestingly, treatment of Hp decreased protein expression of TLR4 while increasing its mRNA expression (Fig. 26). Harald H. et al. has shown that LPS stimulation induced TLR4 trafficking to lysosomes for degradation (Husebye et al., 2006). With regard to binding ability to TLR4, I observed that the level of cell surface TLR4 was decreased by Hp treatment (Fig. 27). Similarly, previous reports showed that upon ligand binding, TLR4 internalizes into endosomes to induce signal transduction by the myeloid differentiation primary response gene 88 (MyD88)-independent pathway, then activates TIR-domain-containing adapter-inducing IFN-β (TRIF) mediated interferon expression (Gomez et al., 2015; Rajaiah et al., 2015). Therefore, internalization of TLR4 from cell surface is necessary to induce IFN-β expression via intracellular signaling activation as I observed. Although, confocal images showed co-localization (Fig. 28), it was unclear whether they interact directly. There is a possibility that the close location of Hp and TLR4 can cause rapid internalization with degradation. Eventually, I found that the

dose-dependent binding of immobilized Hp to TLR4 as LPS binding to TLR4 (Fig. 29).

Numerous factors that regulate bone homeostasis are well established (Sims and Martin, 2014). Therefore, this study demonstrates that inflammatory cytokine-induced Hp secretion in osteoblasts mediates osteoprotective signals that limit excessive osteoclast formation by coupling with osteoclasts (Fig. 35 and 36).

Consistent with Hp playing a role in anti-osteoclast effects, the fundamental role of Hp is to prevent Hb-induced oxidative stress and inflammation. Indeed, human plasma-derived Hp was approved for the treatment of hemolysis, burn injuries, and massive blood transfusions with trauma in 1985 (Schaer et al., 2013). From a biological standpoint, aging showed that processes of osteogenesis and chondrogenesis are reduced during aging while enhancing osteoclastogenesis and adipogenic potential (Cao et al., 2005; Moerman et al., 2004; Zheng et al., 2007). Importantly, Wilson A et al. showed that aging significantly down-regulated Hp transcription in mice-bone marrow derived MSCs (8 to 26 month) (Wilson et al., 2010). This report implies that MSCs express Hp, which is down regulated during aging in bone marrow. Although treatment of Hp to block exorbitant osteoclast activation has not been studied until now, I suggest that Hp is may be clinically useful for protection of bone

from excessive osteoclast activation during aging.

In conclusion, this study unveils a pivotal role of Hp that is secreted by inflammation stimulated-osteoblast, which in turn activates BMMs to produce anti-inflammatory cytokine IFNβ, leading to autonomous regulation of IFNβ that suppresses osteoclast differentiation by TLR4-IFNβ-IFNAR signaling axis. Therefore, I propose that Hp-mediated osteoblast and osteoclast coupling plays a fundamental role in bone protection from excessive osteoclast differentiation.

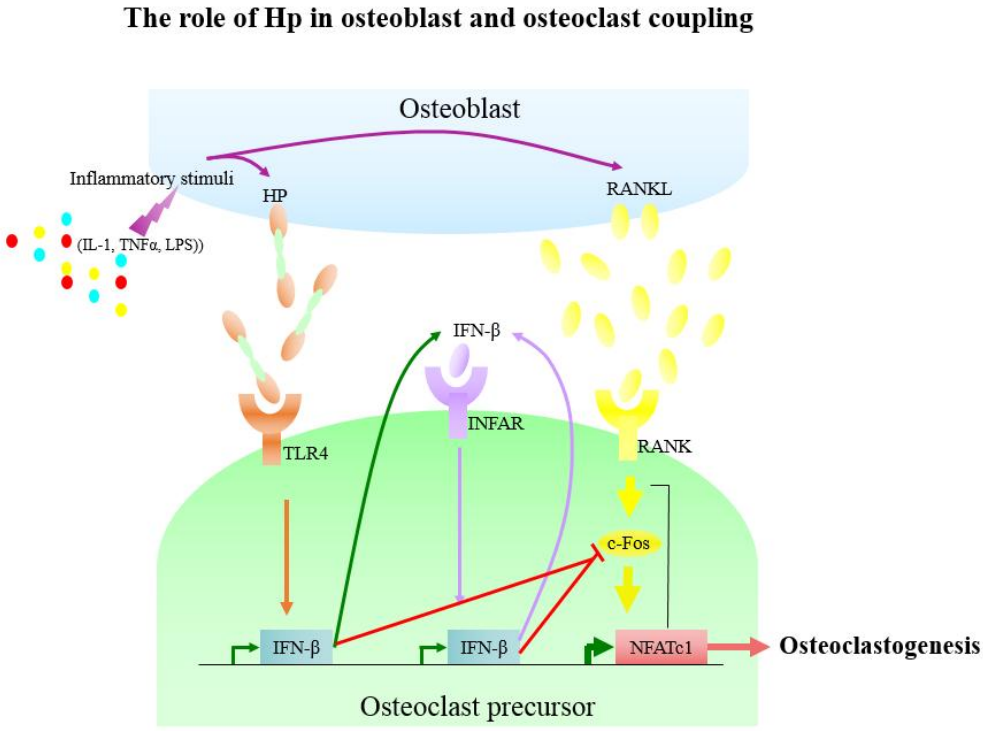

Figure 37. Schematic model of the protective role of Hp on inflammation-induced osteoclastogenesis. Inflammatory cytokines, such as IL-1, TNFα, and LPS stimulate RANKL induction to generate osteoclast differentiation via their receptors RANK-c-Fos-NFATc1 signaling axis. Concurrently secretion of Hp from osteoblast restricts excessive osteoclastogenesis through TLR4-IFNβ signaling activation with autonomous regulation of IFNβ, which results in inhibition of c-Fos to block osteoclast differentiation.

V. References

Arai, F., T. Miyamoto, O. Ohneda, T. Inada, T. Sudo, K. Brasel, T. Miyata, D.M. Anderson, and T. Suda. 1999. Commitment and differentiation of osteoclast precursor cells by the sequential expression of c-Fms and receptor activator of nuclear factor kappaB (RANK) receptors. *J Exp Med*. 190:1741-1754.

Aubry, C., S.C. Corr, S. Wienerroither, C. Goulard, R. Jones, A.M. Jamieson, T. Decker, L.A. O'Neill, O. Dussurget, and P. Cossart. 2012. Both TLR2 and TRIF contribute to interferon-beta production during Listeria infection. *PLoS One*. 7:e33299.

Baldanzi, G., F. Traina, J.F. Marques Neto, A.O. Santos, C.D. Ramos, and S.T. Saad. 2011. Low bone mass density is associated with hemolysis in Brazilian patients with sickle cell disease. *Clinics (Sao Paulo)*. 66:801-805.

Bertaggia, E., G. Scabia, S. Dalise, F. Lo Verso, F. Santini, P. Vitti, C. Chisari, M. Sandri, and M. Maffei. 2014. Haptoglobin is required to prevent oxidative stress and muscle atrophy. *PLoS One*. 9:e100745.

Boyce, B.F., Y. Xiu, J. Li, L. Xing, and Z. Yao. 2015. NF-kappaB-Mediated

Regulation of Osteoclastogenesis. *Endocrinol Metab (Seoul)*. 30:35-44.

Cao, J.J., T.J. Wronski, U. Iwaniec, L. Phleger, P. Kurimoto, B. Boudignon, and B.P. Halloran. 2005. Aging increases stromal/osteoblastic cell-induced osteoclastogenesis and alters the osteoclast precursor pool in the mouse. *J Bone Miner Res*. 20:1659-1668.

Cid, M.C., D.S. Grant, G.S. Hoffman, R. Auerbach, A.S. Fauci, and H.K. Kleinman. 1993. Identification of haptoglobin as an angiogenic factor in sera from patients with systemic vasculitis. *J Clin Invest*. 91:977-985.

Collin-Osdoby, P., L. Rothe, F. Anderson, M. Nelson, W. Maloney, and P. Osdoby. 2001. Receptor activator of NF-kappa B and osteoprotegerin expression by human microvascular endothelial cells, regulation by inflammatory cytokines, and role in human osteoclastogenesis. *J Biol Chem*. 276:20659-20672.

D'Armiento, J., S.S. Dalal, and K. Chada. 1997. Tissue, temporal and inducible expression pattern of haptoglobin in mice. *Gene*. 195:19-27.

de Kleijn, D.P., M.B. Smeets, P.P. Kemmeren, S.K. Lim, B.J. Van Middelaar, E. Velema, A. Schoneveld, G. Pasterkamp, and C. Borst. 2002. Acute-phase protein haptoglobin is a cell migration factor involved in arterial restructuring. *FASEB J*. 16:1123-1125.

do Nascimento, C.O., L. Hunter, and P. Trayhurn. 2004. Regulation of

haptoglobin gene expression in 3T3-L1 adipocytes by cytokines, catecholamines, and PPARgamma. *Biochem Biophys Res Commun*. 313:702-708.

El Ghmati, S.M., E.M. Van Hoeyveld, J.G. Van Strijp, J.L. Ceuppens, and E.A. Stevens. 1996. Identification of haptoglobin as an alternative ligand for CD11b/CD18. *J Immunol*. 156:2542-2552.

Friedrichs, W.E., A.L. Navarijo-Ashbaugh, B.H. Bowman, and F. Yang. 1995. Expression and inflammatory regulation of haptoglobin gene in adipocytes. *Biochem Biophys Res Commun*. 209:250-256.

Gomez, R., A. Villalvilla, R. Largo, O. Gualillo, and G. Herrero-Beaumont. 2015. TLR4 signalling in osteoarthritis--finding targets for candidate DMOADs. *Nat Rev Rheumatol*. 11:159-170.

Ha, H., H.B. Kwak, S.W. Lee, H.M. Jin, H.M. Kim, H.H. Kim, and Z.H. Lee. 2004. Reactive oxygen species mediate RANK signaling in osteoclasts. *Exp Cell Res*. 301:119-127.

Hanasaki, K., L.D. Powell, and A. Varki. 1995. Binding of human plasma sialoglycoproteins by the B cell-specific lectin CD22. Selective recognition of immunoglobulin M and haptoglobin. *J Biol Chem*. 270:7543-7550.

Heinrich, P.C., J.V. Castell, and T. Andus. 1990. Interleukin-6 and the acute

phase response. *Biochem J*. 265:621-636.

Huntoon, K.M., L. Russell, E. Tracy, K.W. Barbour, Q. Li, P.A. Shrikant, F.G. Berger, L.A. Garrett-Sinha, and H. Baumann. 2013. A unique form of haptoglobin produced by murine hematopoietic cells supports B-cell survival, differentiation and immune response. *Mol Immunol*. 55:345-354.

Husebye, H., O. Halaas, H. Stenmark, G. Tunheim, O. Sandanger, B. Bogen, A. Brech, E. Latz, and T. Espevik. 2006. Endocytic pathways regulate Toll-like receptor 4 signaling and link innate and adaptive immunity. *EMBO J*. 25:683-692.

Hussain Mian, A., H. Saito, N. Alles, H. Shimokawa, K. Aoki, and K. Ohya. 2008. Lipopolysaccharide-induced bone resorption is increased in TNF type 2 receptor-deficient mice in vivo. *J Bone Miner Metab*. 26:469-477.

Irie, N., Y. Takada, Y. Watanabe, Y. Matsuzaki, C. Naruse, M. Asano, Y. Iwakura, T. Suda, and K. Matsuo. 2009. Bidirectional signaling through ephrinA2-EphA2 enhances osteoclastogenesis and suppresses osteoblastogenesis. *J Biol Chem*. 284:14637-14644.

Kim, S.D., H.N. Kim, J.H. Lee, W.J. Jin, S.J. Hwang, H.H. Kim, H. Ha, and Z.H. Lee. 2013. Trapidil, a platelet-derived growth factor antagonist, inhibits osteoclastogenesis by down-regulating NFATc1 and suppresses

bone loss in mice. *Biochem Pharmacol*. 86:782-790.

Kodama, H., M. Nose, S. Niida, and A. Yamasaki. 1991. Essential role of macrophage colony-stimulating factor in the osteoclast differentiation supported by stromal cells. *J Exp Med*. 173:1291-1294.

Kristiansen, M., J.H. Graversen, C. Jacobsen, O. Sonne, H.J. Hoffman, S.K. Law, and S.K. Moestrup. 2001. Identification of the haemoglobin scavenger receptor. *Nature*. 409:198-201.

Lacey, D.L., E. Timms, H.L. Tan, M.J. Kelley, C.R. Dunstan, T. Burgess, R. Elliott, A. Colombero, G. Elliott, S. Scully, H. Hsu, J. Sullivan, N. Hawkins, E. Davy, C. Capparelli, A. Eli, Y.X. Qian, S. Kaufman, I. Sarosi, V. Shalhoub, G. Senaldi, J. Guo, J. Delaney, and W.J. Boyle. 1998. Osteoprotegerin ligand is a cytokine that regulates osteoclast differentiation and activation. *Cell*. 93:165-176.

Lee, J.H., H.N. Kim, D. Yang, K. Jung, H.M. Kim, H.H. Kim, H. Ha, and Z.H. Lee. 2009. Trolox prevents osteoclastogenesis by suppressing RANKL expression and signaling. *J Biol Chem*. 284:13725-13734.

Lee, N.K., Y.G. Choi, J.Y. Baik, S.Y. Han, D.W. Jeong, Y.S. Bae, N. Kim, and S.Y. Lee. 2005. A crucial role for reactive oxygen species in RANKL-induced osteoclast differentiation. *Blood*. 106:852-859.

Lisi, S., O. Gamucci, T. Vottari, G. Scabia, M. Funicello, M. Marchi, G. Galli, I.

Arisi, R. Brandi, M. D'Onofrio, A. Pinchera, F. Santini, and M. Maffei. 2011. Obesity-associated hepatosteatosis and impairment of glucose homeostasis are attenuated by haptoglobin deficiency. *Diabetes*. 60:2496-2505.

Maffei, M., I. Barone, G. Scabia, and F. Santini. 2016. The Multifaceted Haptoglobin in the Context of Adipose Tissue and Metabolism. *Endocr Rev*. 37:403-416.

Maffei, M., M. Funicello, T. Vottari, O. Gamucci, M. Costa, S. Lisi, A. Viegi, O. Ciampi, G. Bardi, P. Vitti, A. Pinchera, and F. Santini. 2009. The obesity and inflammatory marker haptoglobin attracts monocytes via interaction with chemokine (C-C motif) receptor 2 (CCR2). *BMC Biol*. 7:87.

Manolagas, S.C., and R.L. Jilka. 1995. Bone marrow, cytokines, and bone remodeling. Emerging insights into the pathophysiology of osteoporosis. *N Engl J Med*. 332:305-311.

Moerman, E.J., K. Teng, D.A. Lipschitz, and B. Lecka-Czernik. 2004. Aging activates adipogenic and suppresses osteogenic programs in mesenchymal marrow stroma/stem cells: the role of PPAR-gamma2 transcription factor and TGF-beta/BMP signaling pathways. *Aging Cell*. 3:379-389.

Moon, J.B., J.H. Kim, K. Kim, B.U. Youn, A. Ko, S.Y. Lee, and N. Kim. 2012.

Akt induces osteoclast differentiation through regulating the GSK3beta/NFATc1 signaling cascade. *J Immunol*. 188:163-169.

Mossman, K.L., M.F. Mian, N.M. Lauzon, C.L. Gyles, B. Lichty, R. Mackenzie, N. Gill, and A.A. Ashkar. 2008. Cutting edge: FimH adhesin of type 1 fimbriae is a novel TLR4 ligand. *J Immunol*. 181:6702-6706.

Nakashima, T., and H. Takayanagi. 2011. New regulation mechanisms of osteoclast differentiation. *Ann N Y Acad Sci*. 1240:E13-18.

Negishi-Koga, T., M. Shinohara, N. Komatsu, H. Bito, T. Kodama, R.H. Friedel, and H. Takayanagi. 2011. Suppression of bone formation by osteoclastic expression of semaphorin 4D. *Nat Med*. 17:1473-1480.

Noppert, S.J., K.A. Fitzgerald, and P.J. Hertzog. 2007. The role of type I interferons in TLR responses. *Immunol Cell Biol*. 85:446-457.

Oh, G.S., H.J. Kim, J.H. Choi, A. Shen, C.H. Kim, S.J. Kim, S.R. Shin, S.H. Hong, Y. Kim, C. Park, S.J. Lee, S. Akira, R. Park, and H.S. So. 2011. Activation of lipopolysaccharide-TLR4 signaling accelerates the ototoxic potential of cisplatin in mice. *J Immunol*. 186:1140-1150.

Orcel, P., M. Feuga, J. Bielakoff, and M.C. De Vernejoul. 1993. Local bone injections of LPS and M-CSF increase bone resorption by different pathways in vivo in rats. *Am J Physiol*. 264:E391-397.

Prowse, K.R., and H. Baumann. 1989. Interleukin-1 and interleukin-6 stimulate

acute-phase protein production in primary mouse hepatocytes. *J Leukoc Biol*. 45:55-61.

Rajaiah, R., D.J. Perkins, D.D. Ireland, and S.N. Vogel. 2015. CD14 dependence of TLR4 endocytosis and TRIF signaling displays ligand specificity and is dissociable in endotoxin tolerance. *Proc Natl Acad Sci U S A*. 112:8391-8396.

Raynes, J.G., S. Eagling, and K.P. McAdam. 1991. Acute-phase protein synthesis in human hepatoma cells: differential regulation of serum amyloid A (SAA) and haptoglobin by interleukin-1 and interleukin-6. *Clin Exp Immunol*. 83:488-491.

Rifkind, J.M., J.G. Mohanty, and E. Nagababu. 2014. The pathophysiology of extracellular hemoglobin associated with enhanced oxidative reactions. *Front Physiol*. 5:500.

Rodan, G.A. 1998. Bone homeostasis. *Proc Natl Acad Sci U S A*. 95:13361-13362.

Rother, R.P., L. Bell, P. Hillmen, and M.T. Gladwin. 2005. The clinical sequelae of intravascular hemolysis and extracellular plasma hemoglobin: a novel mechanism of human disease. *JAMA*. 293:1653-1662.

Sakuma, Y., K. Tanaka, M. Suda, Y. Komatsu, A. Yasoda, M. Miura, A. Ozasa, S. Narumiya, Y. Sugimoto, A. Ichikawa, F. Ushikubi, and K. Nakao.

2000. Impaired bone resorption by lipopolysaccharide in vivo in mice deficient in the prostaglandin E receptor EP4 subtype. *Infect Immun*. 68:6819-6825.

Sato, N., N. Takahashi, K. Suda, M. Nakamura, M. Yamaki, T. Ninomiya, Y. Kobayashi, H. Takada, K. Shibata, M. Yamamoto, K. Takeda, S. Akira, T. Noguchi, and N. Udagawa. 2004. MyD88 but not TRIF is essential for osteoclastogenesis induced by lipopolysaccharide, diacyl lipopeptide, and IL-1alpha. *J Exp Med*. 200:601-611.

Schaer, D.J., P.W. Buehler, A.I. Alayash, J.D. Belcher, and G.M. Vercellotti. 2013. Hemolysis and free hemoglobin revisited: exploring hemoglobin and hemin scavengers as a novel class of therapeutic proteins. *Blood*. 121:1276-1284.

Shen, H., E. Heuzey, D.N. Mori, C.K. Wong, C.M. Colangelo, L.M. Chung, C. Bruce, I.B. Slizovskiy, C.J. Booth, D. Kreisel, and D.R. Goldstein. 2015. Haptoglobin enhances cardiac transplant rejection. *Circ Res*. 116:1670-1679.

Sims, N.A., and T.J. Martin. 2014. Coupling the activities of bone formation and resorption: a multitude of signals within the basic multicellular unit. *Bonekey Rep*. 3:481.

Soysa, N.S., N. Alles, K. Aoki, and K. Ohya. 2012. Osteoclast formation and

differentiation: an overview. *J Med Dent Sci*. 59:65-74.

Takami, M., N. Kim, J. Rho, and Y. Choi. 2002. Stimulation by toll-like receptors inhibits osteoclast differentiation. *J Immunol*. 169:1516-1523.

Takayanagi, H., S. Kim, T. Koga, H. Nishina, M. Isshiki, H. Yoshida, A. Saiura, M. Isobe, T. Yokochi, J. Inoue, E.F. Wagner, T.W. Mak, T. Kodama, and T. Taniguchi. 2002a. Induction and activation of the transcription factor NFATc1 (NFAT2) integrate RANKL signaling in terminal differentiation of osteoclasts. *Dev Cell*. 3:889-901.

Takayanagi, H., S. Kim, and T. Taniguchi. 2002b. Signaling crosstalk between RANKL and interferons in osteoclast differentiation. *Arthritis Res*. 4 Suppl 3:S227-232.

Takayanagi, H., K. Ogasawara, S. Hida, T. Chiba, S. Murata, K. Sato, A. Takaoka, T. Yokochi, H. Oda, K. Tanaka, K. Nakamura, and T. Taniguchi. 2000. T-cell-mediated regulation of osteoclastogenesis by signalling cross-talk between RANKL and IFN-gamma. *Nature*. 408:600-605.

Tseng, C.F., C.C. Lin, H.Y. Huang, H.C. Liu, and S.J. Mao. 2004. Antioxidant role of human haptoglobin. *Proteomics*. 4:2221-2228.

Weitzmann, M.N. 2013. The Role of Inflammatory Cytokines, the RANKL/OPG Axis, and the Immunoskeletal Interface in Physiological

Bone Turnover and Osteoporosis. *Scientifica (Cairo)*. 2013:125705.

Wilson, A., L.A. Shehadeh, H. Yu, and K.A. Webster. 2010. Age-related molecular genetic changes of murine bone marrow mesenchymal stem cells. *BMC Genomics*. 11:229.

Xia, L.X., T. Xiao, H.D. Chen, P. Li, Y.K. Wang, and H. Wang. 2008. Regulation of haptoglobin expression in a human keratinocyte cell line HaCaT by inflammatory cytokines and dexamethasone. *Chin Med J (Engl)*. 121:730-734.

Zhao, C., N. Irie, Y. Takada, K. Shimoda, T. Miyamoto, T. Nishiwaki, T. Suda, and K. Matsuo. 2006. Bidirectional ephrinB2-EphB4 signaling controls bone homeostasis. *Cell Metab*. 4:111-121.

Zheng, H., J.A. Martin, Y. Duwayri, G. Falcon, and J.A. Buckwalter. 2007. Impact of aging on rat bone marrow-derived stem cell chondrogenesis. *J Gerontol A Biol Sci Med Sci*. 62:136-148.

Zou, W., and Z. Bar-Shavit. 2002. Dual modulation of osteoclast differentiation by lipopolysaccharide. *J Bone Miner Res*. 17:1211-1218.

국문초록

파골세포 분화에 대한 합토글로빈의 역할

서울대학교 대학원 세포 및 발생 생물학 전공

(지도교수: 이 장 희)

진 원 종

골 대사 조절에는 골 형성 세포인 조골세포와 골 흡수 세포인 파골세포의 균형적인 활동으로 이루어 지며 골 발생과 골 재생에 주요하게 작용한다. 불균형적인 파골세포의 과도한 골 흡수는 골 밀도를 하락시켜 골다공증, 파제트병, 자가면역관절염 등의 골 질환을

유도하게 된다. 골 환경에서 조골세포로부터 생성되는 시토카인인 M-CSF와 RANKL는 파골세포의 분화를 촉진하고 골 흡수능을 증가시키게 된다. 본 연구는 조골세포에서 발현되는 합토글로빈이 어떤 메커니즘으로 파골세포의 분화를 조절하는지 조사하였다. 마이크로시티를 통한 정량화 분석으로 합토글로빈 유전자가 결손된 실험동물은 파골세포가 증가되고 골 소실을 유발함을 관찰하였다. 세포수준에서 합토글로빈의 자극은 파골세포로의 분화를 억제함을 확인하였고, 파골세포 분화에 필요한 중요 전사인자인 c-Fos와 NFATc1의 발현이 억제되는 것을 확인하였다. 레트로바이러스를 통한 c-Fos 의 과발현은 파골세포 분화에 대한 합토글로빈의 억제효과가 상쇄되는 것을 확인하였다. 합토글로빈으로 인한 전사인자의 발현억제에 인터페론 베타가 관여함을 확인하였고, 인터페론 수용체의 결손은 합토글로빈의 억제효과가 사라지는 것을 관찰하였다. 이로써 합토글로빈은 인터페론 베타를 증가시켜 파골세포 분화에 중요하게 작용하는 c-Fos를 억제하는 메커니즘을 확인하였다. 합토글로빈의 자극으로인한 인터페론 베타의 증가가 어떤 수용체로 통해 일어나는지 확인해본 결과, TLR4가 관여함을 확인하였다. 파골세포의 전구세포인 대식세포와 조골세포의 동시배양조건에서 염증

인자중 하나인 인터류킨1 알파의 자극은 파골세포로의 분화를 유도하게 되는데, 합토글로빈이 결손된 조골세포는 파골세포 분화를 더욱 촉진함을 관찰하였다. 이로써 염증인자로 인해 증가되는 합토글로빈은 과도한 파골세포로의 분화를 억제하는 기능을 갖고 있음을 확인하였다. 위 결과를 토대로 합토글로빈은 조골세포와 파골세포의 적절한 균형을 유지하기 위한 인자로 작용하며, 과도한 파골세포분화로 인한 골 소실 억제에 관여함으로 골의 항상성을 유지함을 확인하였다. 나아가 합토글로빈은 염증환경에서 과도한 파골세포의 골흡수능을 억제할 수 있는 치료제로서의 가능성을 제시한다.

주요어 : 조골세포, 파골세포, 합토글로빈, c-Fos, 인터페론 베타, TLR4

학 번 : 2009-21937